

Super-resolution microscopy with DNA-PAINT

Joerg Schnitzbauer^{1–3}, Maximilian T Strauss^{1–3}, Thomas Schlichthaerle^{1,2}, Florian Schueder^{1,2} & Ralf Jungmann^{1,2}

¹Department of Physics and Center for Nanoscience, Ludwig Maximilian University, Munich, Germany. ²Max Planck Institute of Biochemistry, Martinsried, Germany.

³These authors contributed equally to this work. Correspondence should be addressed to R.J. (jungmann@biochem.mpg.de).

Published online 18 May 2017; doi:10.1038/nprot.2017.024

Super-resolution techniques have begun to transform biological and biomedical research by allowing researchers to observe structures well below the classic diffraction limit of light. DNA points accumulation for imaging in nanoscale topography (DNA-PAINT) offers an easy-to-implement approach to localization-based super-resolution microscopy, owing to the use of DNA probes. In DNA-PAINT, transient binding of short dye-labeled ('imager') oligonucleotides to their complementary target ('docking') strands creates the necessary 'blinking' to enable stochastic super-resolution microscopy. Using the programmability and specificity of DNA molecules as imaging and labeling probes allows researchers to decouple blinking from dye photophysics, alleviating limitations of current super-resolution techniques, making them compatible with virtually any single-molecule-compatible dye. Recent developments in DNA-PAINT have enabled spectrally unlimited multiplexing, precise molecule counting and ultra-high, molecular-scale (sub-5-nm) spatial resolution, reaching ~1-nm localization precision. DNA-PAINT can be applied to a multitude of *in vitro* and cellular applications by linking docking strands to antibodies. Here, we present a protocol for the key aspects of the DNA-PAINT framework for both novice and expert users. This protocol describes the creation of DNA origami test samples, *in situ* sample preparation, multiplexed data acquisition, data simulation, super-resolution image reconstruction and post-processing such as drift correction, molecule counting (qPAINT) and particle averaging. Moreover, we provide an integrated software package, named Picasso, for the computational steps involved. The protocol is designed to be modular, so that individual components can be chosen and implemented per requirements of a specific application. The procedure can be completed in 1–2 d.

INTRODUCTION

For biomedical research, super-resolution microscopy is a promising tool developed in recent years, allowing optical imaging beyond the diffraction limit of light, for up to molecular-scale resolution inside cells. The significance of this group of imaging modalities is underlined by the Nobel Prize in Chemistry in 2014 'for the development of super-resolved fluorescence microscopy'. Super-resolution has been achieved by a variety of imaging modalities, most notably nonlinear structured illumination microscopy (SIM)¹, stimulated emission depletion (STED) microscopy², (fluorescent) photo-activated localization microscopy ((f)PALM)^{3,4} and (direct) stochastic optical reconstruction microscopy ((d)STORM)^{5,6}. All these techniques achieve image resolution beyond the diffraction limit by controlling the state of fluorophores such that only a small subset of them are detectable at any given time. However, super-resolution approaches can be generally divided into the following two groups according to the specific mechanism for controlling the fluorophore state⁷: (i) illumination-pattern-based (SIM and STED) and (ii) single-molecule-localization-based (PALM and STORM) methods. All these super-resolution methods have been successfully used to reveal biological insights^{8–12}, but each has its own advantages and difficulties. A practical advantage of both illumination-based methods is that they do not require specific fluorophores, which makes these techniques straightforward to use for biologists with conventional samples. However, instrumental implementations are typically more complex and intricate. By contrast, the branch of localization-based techniques uses stochastic blinking of specific fluorescent probes. This blinking permits them to be observed one at a time so that their spatial coordinates can be localized with subdiffraction precision¹³. Typically, this blinking is an intrinsic property of fluorescent proteins (PALM) or specific organic dyes (STORM), which can be provoked by specific excitation schemes and buffer conditions^{14,15}. Although instrumentation is typically

simpler for localization-based as compared with illumination-based modalities, the complexity lies in achieving suitable blinking behavior of the dyes. Troubleshooting often means testing a number of parameters such as the choice of dye, labeling density, buffer conditions and excitation illumination, making the blinking a hard-to-control phenomenon. In fact, the choice of 'well-behaving' probes is limited, and further development of substantially improved probes is complex and time-consuming. Moreover, because of the limited choice of probes with appropriate blinking kinetics, photon rates and excitation conditions, multiplexing is still difficult to implement. Furthermore, the complex photophysics of the probes impedes the predictability of blinking events so that quantitative image interpretation is error-prone. Last, owing to limited photon rates and bleaching, optimal localization precision and spatial sampling are still not achieved—the two major factors in resolution¹⁶. Although many biological questions could be addressed with the aforementioned techniques^{8–12}, researchers are still struggling with these complications to truly exploit the power of super-resolution microscopy.

A different route to single-molecule localization microscopy is PAINT¹⁷. Here, instead of labeling target molecules with fixed fluorophores, freely diffusing dyes¹⁷ or dye-labeled ligands (as in uPAINT)¹⁸ target molecules of interest by permanent or transient binding. PAINT is straightforward to implement and does not require special experimental conditions to obtain photoswitching, as long as probes are able to diffuse and reach their target molecules. However, PAINT's original implementation makes it difficult to specifically label a larger variety of biomolecules, as interactions are mainly limited to hydrophobic interactions or electrostatic coupling and are thus difficult to program.

DNA nanotechnology represents a promising tool for utilizing the advantages of the PAINT concept and establishing a programmable target–probe interaction system at the same time.

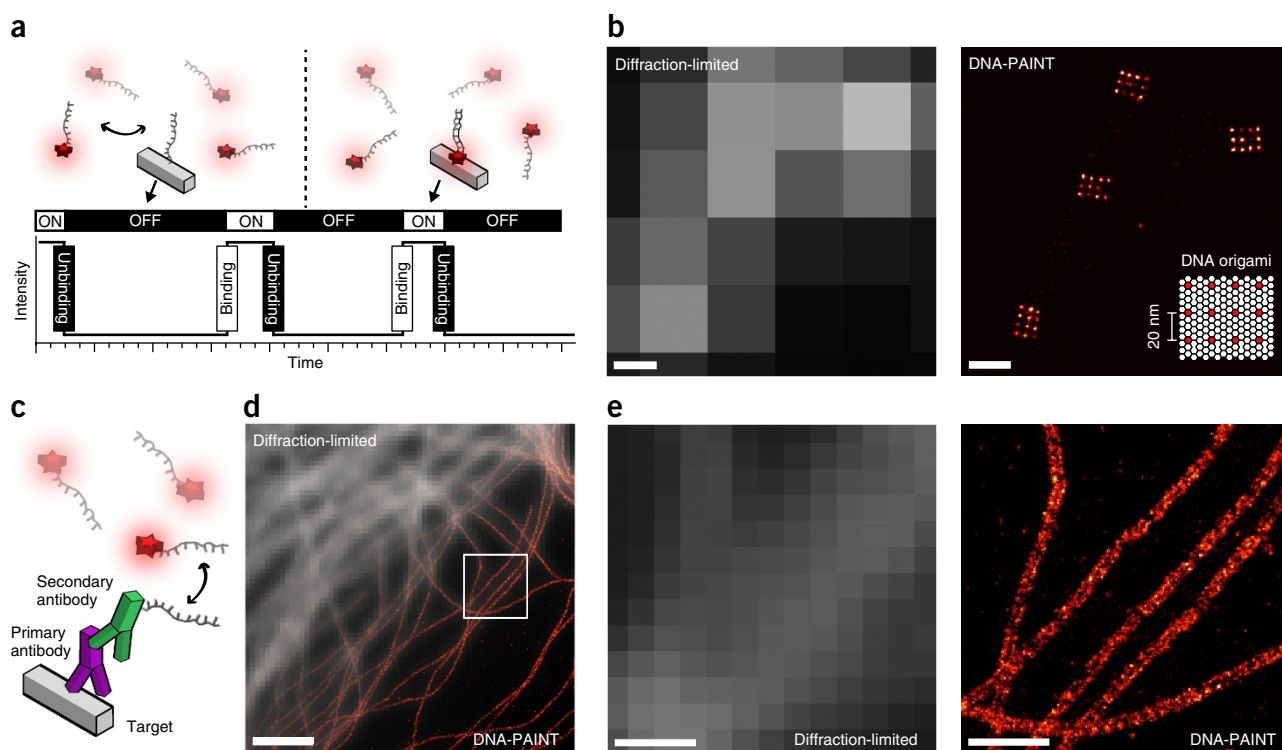


Figure 1 | DNA-PAINT. (a) DNA-PAINT concept. Transient binding of dye-labeled DNA strands (imagers) to their complementary target sequence (docking site) attached to a molecule of interest. The transient binding of imager strands is detected as ‘blinking’, illustrated by the intensity versus time trace. (b) Diffraction-limited (left) and super-resolved DNA-PAINT images (right) of DNA origami nanostructures. Each structure consists of 12 docking strands that are arranged in a 20-nm grid (scheme in lower right corner). (c) *In situ* protein-labeling strategy for DNA-PAINT using primary and DNA-conjugated secondary antibodies. (d) Overlay of a diffraction-limited α -tubulin image (top left) with a super-resolved DNA-PAINT image (bottom right). (e) Close-ups of the highlighted area in d, comparing diffraction-limited image (left) with DNA-PAINT super-resolved image (right). Scale bars, 100 nm (b), 2 μ m (d), 500 nm (e).

Specifically, DNA-based PAINT (DNA-PAINT) has been developed as a straightforward approach to overcome some limitations of current localization-based super-resolution techniques^{19–24}. Similar to the original PAINT concept, DNA-PAINT decouples blinking from dye photophysics, but it also adds the programmability and specificity of using DNA molecules as imaging and labeling probes. A DNA-PAINT system, illustrated in **Figure 1a**, consists of the following two components: a docking strand and an imager strand. These are short, complementary single-stranded DNA oligomers, usually 8–10 nucleotides long. Although the docking strand is fixed to a biological target of interest (e.g., using standard immunolabeling approaches with DNA-conjugated antibodies targeting proteins of interest²⁵ or direct hybridization of docking strands to DNA or RNA molecules), the imager strand is conjugated to an organic dye and diffuses freely in the imaging buffer. Generally, imager strands appear undetectable in the camera because they diffuse over numerous camera pixels during the duration of a single frame. However, owing to their complementary sequence, imager strands can transiently bind to docking strands. During the bound state, imager strands are fixed at the same place for an extended amount of time, allowing the camera to accumulate enough photons from the dye to be detected. The binding duration depends solely on the stability of the formed DNA duplex, and can hence be programmed at will (e.g., by modulating strand length, GC content, temperature or salinity of the imaging buffer). On the other hand, the frequency of binding events is tunable by the influx rate of imager strands

(e.g., by modulating either the concentration of imager strands in the buffer or the association constant). As a result, the user has fine control over the blinking kinetics, which is independent of dye properties or illumination specifics. To date, DNA-PAINT has been used to resolve nanometer-scale structures of DNA origami (**Fig. 1b**), as well as those of cellular proteins, by conjugating docking strands to antibodies (**Fig. 1c–e**).

Advantages and limitations of the method

The properties of DNA-PAINT result in several improvements over more traditional super-resolution approaches. First, the use of DNA-based imaging probes enables high multiplexing by Exchange-PAINT²⁰ that is restricted only by the number of orthogonal DNA sequences, as compared with the spectrally distinct dyes used in classic multiplexing experiments. **Figure 2** illustrates the concept, procedure and results of Exchange-PAINT experiments *in vitro* and *in situ*. When tagging biological targets with orthogonal docking strand sequences, they can be probed sequentially by the respective complementary imager strands (**Fig. 2a**). Specifically, after one DNA-PAINT image has been acquired, the buffer can be exchanged to introduce a different imager strand species. Repeated imaging, washing and reintroduction of new imager strand species then allows researchers to create a multiplexed image of many biological targets. Although we have thus far demonstrated nine-target super-resolution imaging²⁵, multiplexing could reach thousands of species, as the only limitation is the orthogonality of DNA-PAINT sequences.

PROTOCOL

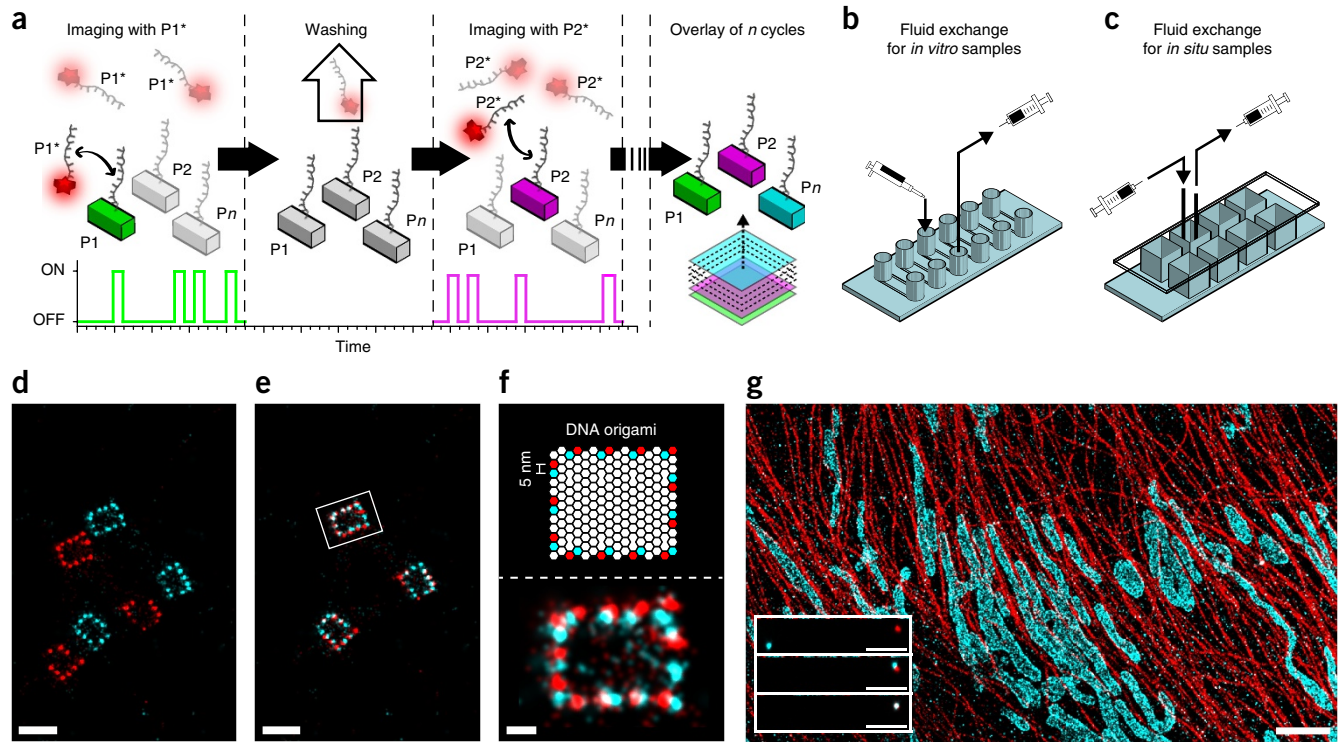


Figure 2 | Exchange-PAINT. (a) Schematic representation of sequential Exchange-PAINT imaging of multiple targets with orthogonal sequences using the same fluorophore. Left to right: $P1^*$ imager strands are in solution and interact with their complementary target sequence, $P1$. After the first acquisition round, the $P1^*$ imager strands are washed away and $P2^*$ imagers are introduced to image the next target. This is then repeated for the remaining target cycles, and pseudocolors are assigned for each respective imaging round. Last, all rounds are aligned and overlaid to form the final multiplexed Exchange-PAINT image of n targets. (b) Fluid exchange chamber for *in vitro* samples (e.g., for DNA origami imaging). Liquid is introduced by pipetting into the inlet. The outlet is attached to a syringe with a flexible tube to remove the liquid. (c) Fluid exchange chamber for *in situ* samples (i.e., used for *in situ* cellular imaging). Two tubes with syringes are connected to an 8-well chambered cover glass to facilitate fluid exchange. (d) Two rounds ('colors') Exchange-PAINT image of a frame-like DNA origami structure carrying two orthogonal docking strand species (red and cyan; see also f, for design schematics). (e) Pseudocolor image after alignment of the imaging rounds using Picasso's automated align function. (f) Top: DNA origami design. Bottom: Close-up (white box from e) of one frame-like structure. The distance between red and blue handles is ~ 5 nm. (g) *In situ* Exchange-PAINT image of protein targets α -tubulin (red) and Tom20 (cyan) with two primary and DNA-conjugated secondary antibody sandwiches. Inset: Images of one alignment marker (gold nanoparticle) in each Exchange-PAINT round without channel alignment (top), after Picasso's automated cross-correlation analysis (middle) and after manually selecting the particle as an alignment fiducial (bottom). Scale bars, 100 nm (d, e), 20 nm (f), 2 μ m (g), 300 nm (g, insets).

Second, the predictability and tunability of DNA binding and unbinding events, combined with effectively nonexistent bleaching, allow for accurate quantitative image interpretation (i.e., counting of single molecules in an integer manner), implemented in quantitative PAINT (qPAINT)²². **Figure 3** depicts the qPAINT concept, procedure and results. A more detailed description of the method will be given below.

Third, DNA-PAINT simplifies the selection of suitable dyes for imaging, as the parameter space is reduced from rather complex photophysical properties (e.g., switching behavior) to basically a single parameter—the photon budget. This also means that DNA-PAINT can use a large pool of existing fluorophores that were previously not applicable to localization-based super-resolution microscopy.

Finally, by programming the binding duration, an extremely high number of photons can be detected from a single binding (or blink) event, enabling optimal localization precision. The only limitations regarding the achievable photon budget are experimental time and photobleaching during a single binding event. However, the latter can be greatly reduced by specific imaging buffer compositions, such as oxygen-scavenging systems

and triplet-state quenchers^{26–28}. Even if bleaching of individual dyes does occur, it has only a minimal detrimental effect overall, because of the practically infinite supply of replenishable 'fresh' imager strands from solution. All things considered, photobleaching—which is a considerable complication for all other super-resolution techniques—is eliminated as a restriction on achieving optimal sampling of the biological structure under investigation. Such optimized experimental conditions for high localization precision, combined with intricate drift correction methods, enable imaging at thus far unprecedented resolution in optical microscopy, for the first time enabling true molecular-scale resolution²³, which, to our knowledge, has not been achieved using any other super-resolution method. Example results of images with localization precisions of ~ 1 nm, yielding resolution better than 5 nm, and intermediate results of the applied drift correction are shown in **Figure 4**. To achieve these results, a large number of DNA origami structures were used as drift markers, considering first the whole structure, followed by the use of individual DNA-PAINT binding sites as fiducials. To eventually translate the *in vitro* ultra-resolution achievements to *in situ* samples such as fixed cells, a key challenge is the labeling

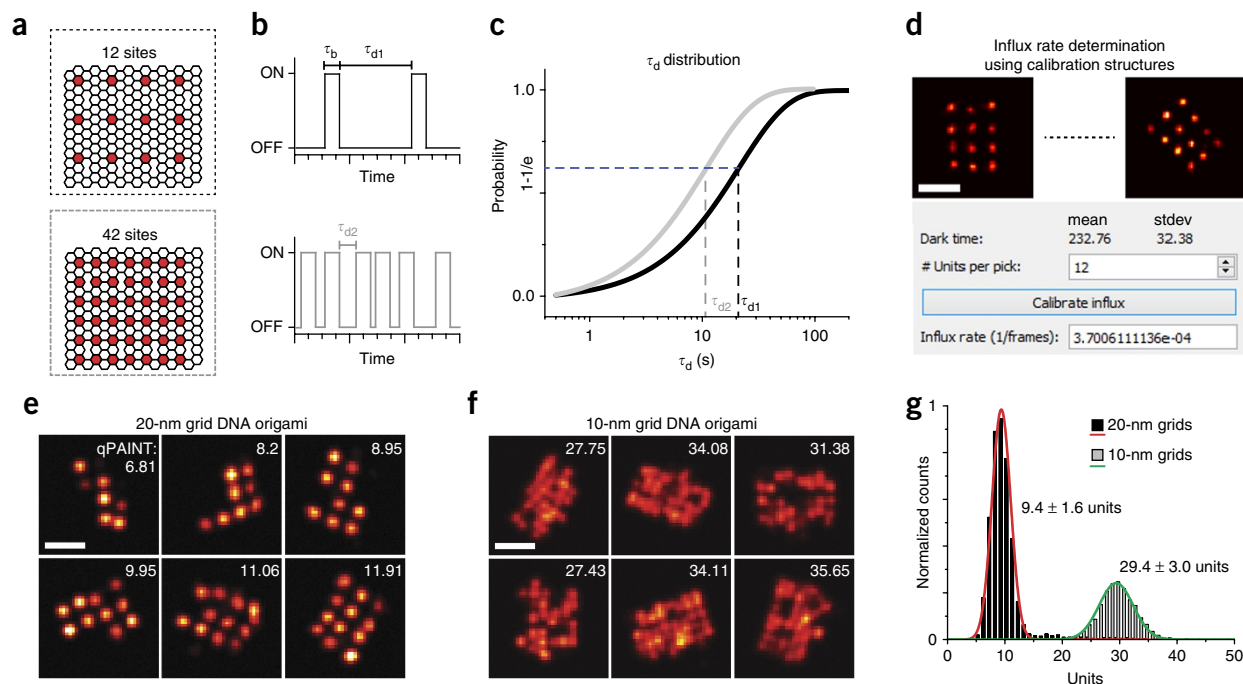


Figure 3 | qPAINT. (a) Design schematics for two DNA origami structures with 12 target sites spaced 20 nm apart (top, black-dotted box) and 42 binding sites spaced 10 nm apart (bottom, gray-dotted box), respectively. (b) DNA origami structures with 12 binding sites (top) exhibit fewer binding (blinking) events as compared with structures with 42 binding sites (bottom), resulting in longer dark times (τ_{d1}) and shorter dark times (τ_{d2}) for the 20-nm grids and 10-nm grids, respectively. (c) Mean dark times τ_{d1} and τ_{d2} are obtained by fitting the cumulative distribution function of the dark times. (d) To measure binding sites for a structure of interest, DNA origami nanostructures are used to calibrate the influx rate (here displayed as the number of blinks per frame). Visual inspection of the DNA origami defines the units (or binding sites) per pick (here only origami displaying 12 binding sites are picked for calibration, top) and can be used to calculate the influx rate (Picasso software dialog, bottom). (e) Visual inspection of 20-nm-grid DNA origami structures in comparison with qPAINT-predicted binding sites after calibration shows good agreement. (f) Visual comparison of 10-nm-grid DNA origami with predicted binding sites via qPAINT. (g) Histogram distribution of binding sites for 20-nm-grid structure (black and red, $n = 4,210$) in comparison with 10-nm-grid structure (gray and green, $n = 1,818$). Scale bars, 50 nm.

probe size. The size of the labeling probes introduces a linkage error and effectively limits the labeling density (because of sterical hindrance). Both these effects finally limit the achievable resolution. One way to address these issues in cells could be the use of smaller labeling agents such as nanobodies²⁹ or aptamers³⁰, rather than antibodies.

Although DNA-PAINT offers several advantages over traditional super-resolution techniques, as discussed above, we also note that there are currently limitations. One disadvantage is the fact that ‘imager’ strands are nonfluorogenic, with the following two implications: first, DNA-PAINT is limited to optical sectioning techniques such as total internal reflection (TIR), oblique³¹ or light-sheet³² illumination because of elevated background fluorescence originating from unbound imager strands. Second, the nonfluorogenic nature of imager strands furthermore sets an upper limit to the achievable image acquisition speed as compared with those of STED, PALM, STORM or SIM. Furthermore, DNA-PAINT applications are currently limited to fixed specimens. Live-cell imaging could be more difficult to achieve as compared with the aforementioned techniques, because of the complexity of infusing dye-labeled nucleic acid strands into living cells and the unforeseen consequences of introducing nucleic acids in general. However, we note that DNA-PAINT applications to molecules on cell surfaces such as membrane-bound receptors should be feasible even for living cells.

All in all, the DNA-PAINT imaging framework greatly reduces many technical difficulties of localization-based super-resolution microscopy and opens up possibilities for new technical development and biological applications. It will therefore allow many research groups to address their biological question with much greater efficiency. To ease the adoption of DNA-PAINT for novice and expert researchers in the super-resolution field, this protocol details the involved procedures and provides an integrated software package, named Picasso, which is specifically designed for DNA-PAINT applications. Except for data acquisition, Picasso can handle all computational efforts required in this protocol, including *in silico* data simulation, DNA origami design, and basic and advanced functionality for localization-based super-resolution microscopy.

Overview of the main procedures

The overarching goal of this protocol is to enable both novices and expert users to quickly obtain high-quality DNA-, Exchange-PAINT and qPAINT imaging data *in silico*, *in vitro* and *in situ*, without prior expertise in super-resolution microscopy. Here, we are using the term *in vitro* for DNA-PAINT studies with DNA origami structures on BSA/biotin/streptavidin-coated glass slides. By contrast, *in situ* is used to describe experiments involving fixed-cell samples. The protocol is based on several studies^{19,20,22,23,25} and is arranged into four major sections, as illustrated in **Figure 5**: sample

PROTOCOL

preparation (*in vitro* and *in situ*), data acquisition, image reconstruction and image post-processing. For sample preparation, we describe the following two procedures: *in vitro* imaging (i.e., of DNA origami nanostructures) (Steps 1–18; **Box 1**) and *in situ*

imaging (i.e., of cell samples) (Steps 19–33). Although not covered in this protocol, the procedures could be adjusted for DNA-PAINT imaging in tissue or whole organisms. Subsequently, we explain data acquisition (Steps 34–49), including a detailed procedure

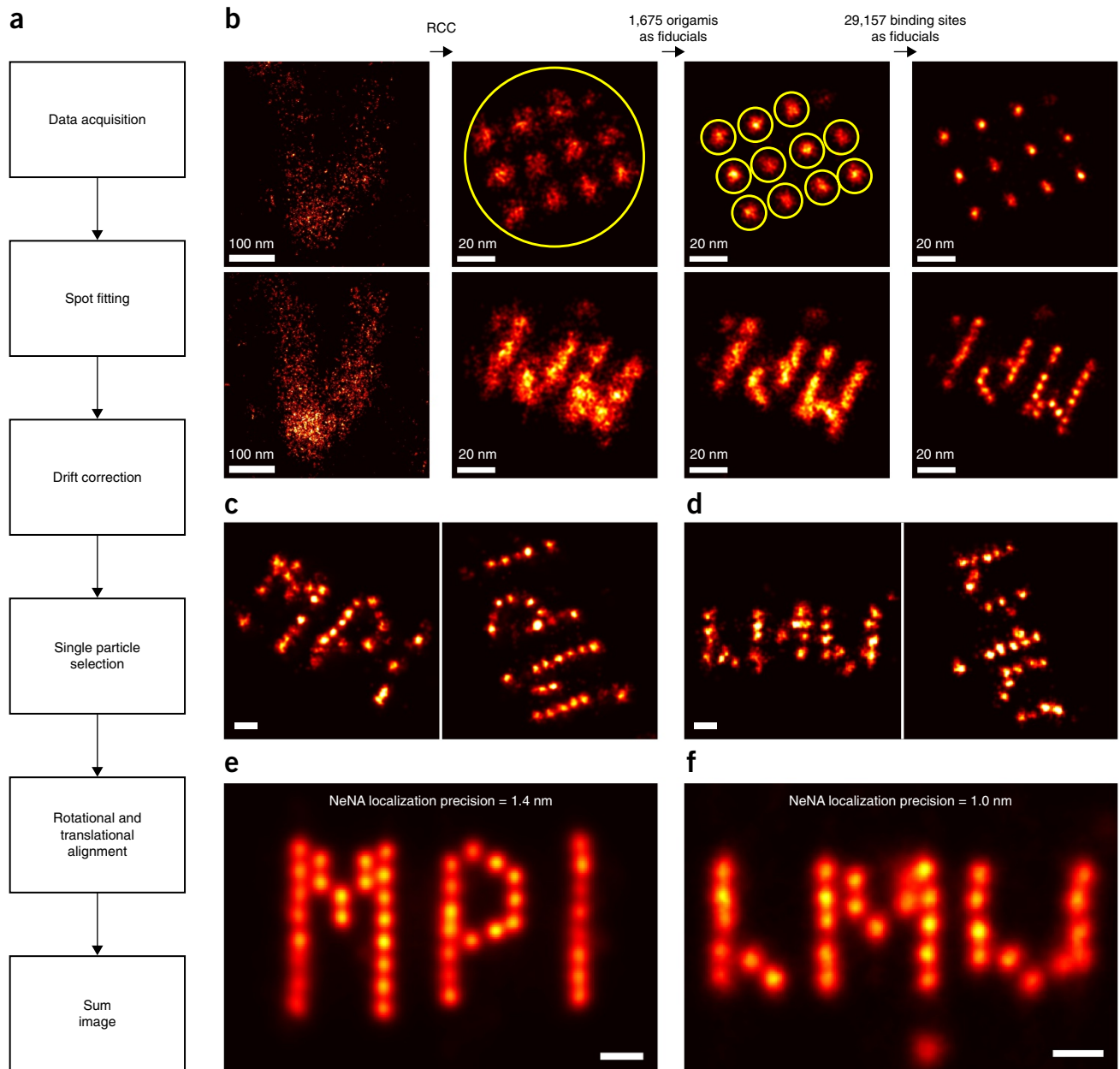


Figure 4 | ‘Ultra-resolution’ with DNA-PAINT. (a) Workflow for ultra-resolution imaging with advanced drift correction and particle averaging. (b) Multistage drift correction with Picasso. Top: 20-nm-grid DNA origami structures used as reference structures and drift markers. Bottom: DNA origami target structure (designed to display the letters ‘MPI’ (upside down) with 5-nm ‘docking strand resolution’) present in the same sample as the 20-nm origami. In the first drift correction stage, an RCC procedure is applied to the whole field of view (image column after RCC arrow shows results). The second step uses Picasso’s semiautomated particle pick function (picked structure visualized by yellow circle) to select 1,675 DNA origami structures as fiducials for drift correction (drift for all structures is globally averaged and subtracted from the localization data). The result for this step is depicted in the third column. The third and last iteration uses the individual binding sites of the 20-nm grid for drift correction. Here, 29,157 binding sites were used as fiducial markers. The resulting image for the MPI target structures shows clearly resolved single binding sites spaced 5 nm apart. (c) Selection of two MPI origami after drift correction. Localization clusters of individual DNA-PAINT binding sites with a distance of ~5 nm are well resolved and circular, indicating that the residual drift is minimal and rotationally invariant. (d) Selection of two DNA origami, designed to show the letters ‘LMU’, from a different sample than in **b,c,e**, but after an analogous drift correction as shown in **b**. The images demonstrate minimal residual drift similar to that of the MPI structures shown in **c**. (e) Average image of 295 DNA origami with the letters ‘MPI’. The mean number of localizations in individual images is $3,485 \pm 1,197$. All DNA-PAINT binding sites are visible, even though individual images miss binding sites because of incomplete strand incorporation, as seen in **c**. (f) Average image of 215 DNA origami with the letters ‘LMU’. The mean number of localizations in the individual images is $2,323 \pm 436$. Scale bars, 10 nm (**c–f**).

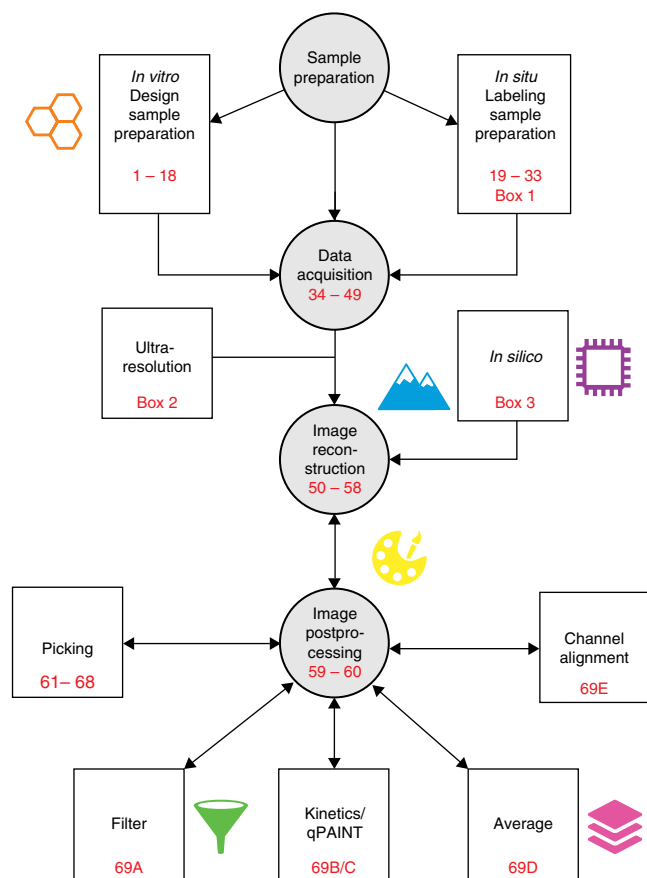


Figure 5 | DNA-PAINT protocol workflow. Starting with sample preparation, the user can perform either *in vitro* or *in situ* experiments. Next, data acquisition is performed (parameters for ‘Ultra-resolution’ are described in **Box 2**). The user may additionally generate DNA-PAINT data by *in silico* simulations. During image reconstruction, single-molecule fluorescence spots are localized, and resulting super-resolution images are visualized with ‘Picasso: Render’. Image post-processing focuses first on drift-correction procedures. Then, special emphasis is given to analyzing the localization-based DNA-PAINT data through picking regions of interest, performing kinetic and qPAINT analysis, averaging images for ultra-resolution analysis and channel alignment for Exchange-PAINT or filtering of the localization list. Program icons indicate in which Picasso component the respective step is performed—hexagons: ‘Design’; microchip: ‘Simulate’; mountain peaks: ‘Localize’; paint palette: ‘Render’; funnel: ‘Filter’; stacked layers: ‘Average’. The Picasso program icons are based on contributions from the Noun Project (<https://thenounproject.com>)—‘Design’: hexagon by Creative Stall; ‘Simulate’: microchip by Futishia; ‘Localize’: mountains by Montana Ruboco; ‘Filter’: funnel by José Campos; ‘Render’: paint palette by Vectors Market; ‘Average’: layers by Creative Stall.

to achieve very high spatial resolution (<5 nm) with DNA-PAINT, which requires particular care in sample preparation and data acquisition (**Box 2**). Furthermore, we lay out the procedure to simulate typical DNA-PAINT data *in silico* for test and optimization purposes (**Box 3**). Then, image reconstruction is explained in two steps: fitting of single-molecule spots and subsequent rendering of the super-resolution image (Steps 50–58). Finally, we describe multiple procedures for post-processing such as drift correction (Steps 59 and 60), selection of regions of interest (Steps 61–68), filtering of localizations (Step 69A), quantitative imaging with qPAINT (Step 69B and C), particle averaging (Step 69D) and channel alignment for multiplexed images (Step 69E). Additional

steps required for multiplexed imaging with Exchange-PAINT are described as optional steps in the respective sections.

One of the defining components of this protocol for DNA-PAINT is an integrated software package called Picasso, which enables researchers to quickly obtain meaningful reconstructed image results without the need of additional third-party software tools.

The Picasso software package

Like similar localization-based super-resolution methods, DNA-PAINT requires intricate data analysis. For that matter, we provide an integrated software package named ‘Picasso’ (free to download from <http://www.jungmannlab.org>). Although Picasso is suitable for any localization microscopy technique, it provides specific support for DNA-PAINT applications, e.g., qPAINT. All computational steps described in this protocol can be performed with Picasso. This includes designing of DNA origami structures and simulating typical DNA-PAINT data. After installation, Picasso is available as several stand-alone (but interlinked) modular components with graphical user interfaces. The components are named ‘Design’, ‘Simulate’, ‘Localize’, ‘Filter’, ‘Render’ and ‘Average’. The ‘Design’ component allows the user to visually design rectangular 2D DNA origami structures, which we call Rothmund’s rectangular origami (RRO)³³, with DNA-PAINT handles. For that matter, ‘Design’ autogenerates order lists and pipetting instructions. With ‘Simulate’, the user may generate typical DNA-PAINT raw data from *in silico* simulations. After data have been acquired or simulated, the ‘Localize’ component allows the user to identify and fit the coordinates of single-molecule spots. ‘Picasso: Filter’ offers a convenient tool to inspect the localization list, plot histograms of localization properties and filter localizations with undesired properties. Super-resolution images can be rendered and inspected with the Picasso component ‘Render’. ‘Picasso: Render’ also offers various post-processing functions such as advanced drift correction and quantitative image evaluation by qPAINT. Last, the ‘Average’ module provides the functionality to perform particle averaging (i.e., rotational and translational alignment) of multiple images of the same structure. Analogous to single-particle reconstruction in the electron microscopy field, this procedure helps to improve the signal-to-noise ratio of images. Overviews of the graphical user interfaces for the ‘Design’, ‘Simulate’, ‘Localize’, ‘Render’ and ‘Filter’ components are shown in **Supplementary Figures 1–5**.

Although in principle a cross-platform development, we currently supply a one-click installer of Picasso for Microsoft Windows 64-bit operating systems. This single executable setup file can be downloaded from our website at <http://www.jungmannlab.org>. Picasso is developed in Python, and the source code is available at <https://github.com/jungmannlab/picasso>.

Design and preparation of DNA origami structures

As DNA-PAINT makes use of the programmability of (transient) DNA strand hybridization to enable super-resolution imaging, DNA-based objects are convenient *in vitro* test targets for imaging. Nucleic acids can serve as powerful building blocks for nanometer-scale structures based on sequence-guided self-assembly, which is the foundation of structural DNA nanotechnology^{34,35}. DNA origami are complex, self-assembled, 2D or 3D structures created by annealing DNA strands of specifically designed sequences³³. In DNA origami, a long single-stranded DNA

Box 1 | Construction of a fluid exchange chamber for *in situ* imaging

● TIMING 30 min

Procedure

For *in situ* Exchange-PAINT experiments, we recommend a simple, custom-built fluid exchange system. The lid of an 8-well chambered cover glass can be modified with one inlet and one outlet, which can be connected to imaging and washing buffer reservoirs by silicone tubing. The modified lid can be used for multiple imaging experiments, although the connected tubing should be thoroughly cleaned before reuse. Using a syringe, flush at least 3 ml (as reference for 1-m tubing with a 1.5-mm diameter; adjust accordingly) of H₂O, followed by 3 ml of 80% EtOH and finally 3 ml of H₂O, through the tubing. Follow these instructions to prepare such a lid:

1. Drill two holes with a diameter of 1.5 mm into the lid of an 8-well chambered cover glass, so that two needles can penetrate it.
2. Use a rotary tool with cutting disc or equivalent to remove the syringe connectors from two 1.2 × 40-mm needles. Alternatively, use a side cutter (although this could potentially lead to a 'less clean cut') and squeeze the channel shut. To reopen, carefully apply pressure with the side cutter at the side of the cut. Make sure that the needle is at least 2.5 cm long to be able to reach the bottom of the chambered cover glass.

! **CAUTION** Handle the needles with care and do not puncture yourself.

3. Cut away the sharp end of one of the needles, so the channel can reach the bottom of the wells. Carefully apply pressure to open the metallic channel of the needle at the cut side with the side cutter.

! **CAUTION** Handle the needles with care and do not puncture yourself.

4. Connect the cut needles to ~50 cm of tubing. Make sure that the tubing is long enough that there is enough space to handle the liquids and syringes at the microscope. To connect the tubing to the syringes, use 1.1 × 40-mm needles on the other end of the tubing.
 - ▲ **CRITICAL STEP** The length of the tubing depends heavily on the accessibility of the microscope; adjust the tubing length for proper handling.

5. For imaging, fix the tubing to the microscope body via tape.

▲ **CRITICAL STEP** Leakage could lead to damage of the microscope. Check all tubing and connections before use.

molecule (called the 'scaffold', derived from M13mp18 single-stranded phage DNA) is folded into a desired shape by ~200 short, single-stranded DNA strands (called 'staples'). Each staple has a defined sequence and specifically binds certain parts of the scaffold together. Structures are usually assembled in a one-pot reaction using thermal annealing. After the self-assembly is completed, the scaffold is 'folded' into the desired shape with the staple strands at prescribed positions in the final origami.

The rather complex and time-consuming procedure of manually designing DNA origami structures has been markedly simplified by computer-aided design tools, such as the freely available caDNAno³⁶ and vHelix³⁷ packages, as well as by simulation programs such as CanDo³⁸. Furthermore, folding protocols for structure formation are now optimized for structure yield and folding speed^{39–41}. In addition, several methods for subsequent purification of DNA nanostructures from unwanted excess of staple strands are described in the literature, such as agarose gel purification⁴², rate-zonal centrifugation⁴³ or PEG purification⁴⁴.

One of the early applications of DNA origami was its use as a microscopy standard in the form of a self-assembled nanoruler⁴⁵. Owing to the unique positioning accuracy of DNA origami and its excellent structural integrity, the structures present an ideal platform to directly validate imaging methods and compare instrumentation. Specifically, they are a valuable tool in calibrating fluorescence and super-resolution microscopes⁴⁶.

Although it is possible to create a wide range of structures with the DNA origami technique, some are more suitable for use as a reference structure with DNA-PAINT than others. In this protocol, we use a flat, rectangular 2D DNA origami structure, adapted from the one originally described³³, here referred to as RRO. With dimensions of 90 × 70 nm and, in our case, 176 freely addressable staples arranged in a hexagonal lattice with 5-nm spacing,

it is an ideal structure for DNA-PAINT imaging (see Fig. 1b as an example). For surface immobilization, the structure is modified with eight biotinylated staple strands that can bind to a BSA–biotin–streptavidin-coated glass surface.

'Picasso: Design' is an essential tool in this protocol that reduces all design steps to a minimum. Figure 6 shows screenshots and outlines the procedure for creating DNA origami, from design to purification. For a detailed overview of the graphical user interface, refer to **Supplementary Figure 1**. The program displays a hexagonal lattice that serves as a canvas representing all possible staple positions available for modification in the RRO structure. It features a 'point-and-click' approach, so that the desired pattern can be made by simply 'painting' on the canvas. Clicking a hexagon will fill it with a previously selected color; each color corresponds to a built-in staple extension on the 3'-end. As all modifications are just staple extensions of the RRO structure, the core sequences are not altered, and time-consuming tasks such as altering the routing of staples or modifying their base sequence are not necessary. In addition, 'Picasso: Design' automatically calculates folding recipes for a given design based on optimized excess rates for the RRO and creates visual pipetting aids for 96-well plates so that pipetting of staple mixes is greatly facilitated. In consequence, the creation of DNA origami reference structures for DNA-PAINT can be achieved in the most straightforward way.

In situ sample preparation

A unique advantage of fluorescence microscopy, making it one of the preferred characterization tools in biological research, is its ability to interrogate biomolecules of interest, such as proteins or nucleic acids, with high efficiency and specificity. Generally, fluorescent labeling of target molecules is achieved either by

Box 2 | Ultra-resolution imaging ● TIMING ~7 h

Procedure

To achieve ultra-resolution (<5 nm), imaging conditions must be carefully adjusted. The key to higher spatial resolution is to extract more photons per frame from a blinking event while simultaneously keeping the background low. This can be achieved by optimizing the laser excitation power, as well as the fluorescence ON time (and adjusting the integration time accordingly). The background can be reduced, for example, by decreasing the imager concentration. In this case, the acquisition time should be increased to ensure proper sampling of the target structure. However, with an imager concentration that is too low, drift correction might become less accurate owing to the smaller number of localizations per frame. We also want to note that the number of drift markers in a field of view should be as high as possible, to ensure precise drift correction. One way to achieve this is to make use of the larger field of view obtainable with today's sCMOS cameras. For advanced drift correction, a 20-nm and a 10-nm grid DNA origami should be used as fiducials. Furthermore, oxygen-scavenging systems, such as the PCA/PCD/Trolox (PPT) system, allow the harvesting of more photons as they increase fluorophore stability²⁷. The following steps describe in detail how to achieve ultra-resolution for imaging DNA origami structures.

1. Design and fold DNA origami structures for ultra-resolution imaging—e.g., the LMU or MPI logo. In addition, fold 20-nm and 10-nm grid DNA origami for use as drift markers (see Steps 1–17).
2. Prepare the oxygen-scavenging system PPT at least 1 h before imaging.
3. Prepare a sample with the target structure and DNA origami drift markers (see Step 18) using the following parameters:
 - Origami solution ratio: 1/4 target structure (i.e. LMU or MPI logo), 1/4 20-nm drift marker, 1/4 10-nm drift marker and 1/4 Buffer B+
 - Imager concentration (with PPT): 0.5 nM–1 nM.
4. Follow steps 34–48 with the following adjustments: 350 ms exposure time, 80,000 total number of frames. Set the excitation power density to ~4.5 kW/cm² at the sample plane.

genetically fusing a protein tag to the target⁴⁷ or by attaching an external binder molecule during a staining procedure—e.g., dye-labeled antibodies⁴⁸. For DNA-PAINT, the labeling requirement is that a DNA docking strand is attached to the target. Although a variety of strategies could be feasible for that^{29,30,49–52}, this protocol focuses on immunostaining with DNA-conjugated antibodies²⁵. Specifically, we describe how antibodies can be chemically modified and used for *in situ* DNA-PAINT imaging of fixed cells (Steps 19–33).

The concept of *in situ* DNA-PAINT with primary and secondary antibody labeling is shown in **Figure 1c**: imager strands from solution transiently bind to handle sites on the secondary antibody. Imaging results for *in situ* samples prepared with antibody labeling are shown in **Figure 1d,e**, displaying a gradient overlay of diffraction-limited microtubules in comparison with the reconstructed super-resolved image. Furthermore, **Figure 2g** shows DNA DBCO-labeled antibody staining of Tom20, located mainly at the outer mitochondrial membrane, and DNA thiol-labeled antibody staining of microtubules.

Various avenues are possible for attaching DNA strands to antibodies, including biotin–streptavidin linkage²⁰ or covalent attachment of the DNA to the antibody^{22,53,54}. Although biotin–streptavidin linkage was used in the initial *in situ* DNA-PAINT demonstration²⁰, we here discuss a covalent attachment strategy, which was used in subsequent work²² similar to previously reported strategies for DNA–protein conjugation^{53,54}. Here, an NHS ester linker is covalently attached to amino groups on the antibody and to certain functional groups on the DNA, such as reduced thiols²², azides^{53,55}, alkynes⁵³ or DBCO⁵⁵, for click chemistry. This results in cross-talk-free attachment, as well as smaller linker sizes between antibody and DNA strand, as compared with the biotin–streptavidin linkage²⁰.

Depending on the target molecules under investigation, it is furthermore important to evaluate different fixation strategies.

For example, structural proteins, such as actin filaments or microtubules, can be fixed with pre-extraction and glutaraldehyde to decrease background and preserve structural integrity⁵⁶. However, structural artifacts can arise from the various fixation strategies. For an in-depth discussion of fixation artifacts, we refer to a recent article by Whelan *et al.*⁵⁷. DNA-PAINT was also applied to tissue samples, as was recently shown in *Drosophila* embryos²², generally following the same procedures as described here. However, we do note that potential changes to the herein described protocol for more complex tissue samples might become necessary.

Data acquisition

A multitude of acquisition software packages are available for performing localization-based super-resolution microscopy, in particular for commercial microscope setups. In this protocol, we describe our procedures based on the freely available open-source acquisition software μ Manager⁵⁸. μ Manager is used in a wide range of microscopy areas and offers broad device support for microscope bodies, cameras and peripherals. The Picasso software suite is specifically designed to be compatible with μ Manager.

Currently, two types of cameras are typically used in the field of single-molecule localization-based imaging—scientific complementary metal oxide semiconductor (sCMOS)- and electron-multiplying charge coupled device (EMCCD)-based cameras. sCMOS cameras provide better temporal resolution because of their faster readout electronics, resulting in a larger optical field of view as compared with EMCCDs under similar conditions. EMCCD cameras, in comparison, provide better quantum yields in low-light applications and thus higher signal-to-noise ratios⁵⁹. As DNA-PAINT provides comparably higher signal-to-noise ratios (SNRs), both camera types are suitable in this context.

It has been shown that a pixel-dependent noise calibration for sCMOS cameras can improve localization precision in STORM⁶⁰. However, for DNA-PAINT experiments—including the

Box 3 | *In silico* simulation of DNA-PAINT data ● TIMING 10–60 min

Picasso’s simulation module (‘Picasso: Simulate’) is a tool for evaluating experimental conditions for DNA-PAINT and generating ground-truth data for test purposes. This allows systematic analysis of how different experimental parameters such as imager concentration, target density or integration time influence the imaging quality and whether the target structure can be resolved with DNA-PAINT. By default, ‘Picasso: Simulate’ starts with preset parameters that are typical for a DNA-PAINT experiment. Thus, meaningful raw DNA-PAINT data can be readily simulated for a given input structure without the need of a super-resolution microscope. The simulation output is a movie file in .raw format, as it would be generated during an *in vitro* DNA-PAINT experiment on a microscope.

Procedure

1. Start ‘Picasso: Simulate’.
2. Define the number and type of structures that should be simulated in the group ‘Structure’. Predefined grid- and circle-like structures can be readily defined by their number of columns and rows, or their diameter and the number of handles, respectively. Alternatively, a custom structure can be defined in an arbitrary coordinate system. To do so, enter comma-separated coordinates into ‘Structure X’ and ‘Structure Y’. The unit of length of the respective axes can be changed by setting the spacing in ‘Spacing X,Y’. For each coordinate point, an identifier for the docking site sequence needs to be set in ‘Exchange labels’ as a comma-separated list. Correctly defined points will be updated live in the ‘Structure [nm]’ window. Note that entries with missing x coordinate, y coordinate or exchange label will be disregarded. When a structure has been previously designed with ‘Picasso: Design’, it can be imported with ‘Import structure from design’. A probability for the presence of a handle can be set with ‘Incorporation’. By default, all structures are arranged on a grid with boundaries defined by ‘Image size’ in ‘Camera parameters’ and the ‘Frame’ parameter in the ‘Structure’ group. ‘Random arrangement’ distributes the structures randomly within that area, whereas ‘Random orientation’ rotates the structures randomly. Selecting the button ‘Generate positions’ will generate a list of positions with the current settings and update the preview panels. A preview of the arrangement of all structures is shown in ‘Positions [Px]’, whereas an individual structure is shown in ‘Structure [nm]’.
3. The group ‘PAINT Parameters’ allows adjustment of the duty cycle of the DNA-PAINT imaging system. The mean dark time is calculated by $\tau_d = (k_{on} \cdot c)^{-1}$. The mean ON time in a DNA-PAINT system is dependent on the DNA duplex properties. For typical 9-bp imager/docking interactions, the ON time is ~500 ms. ON times can be experimentally estimated with Picasso as described in Step 69B.
4. In ‘Imager Parameters’, fluorophore characteristics such as PSF width and photon budget can be set. Adjusting the ‘Power density’ field affects the simulation analogously to changing the laser power in an experiment.
5. The ‘Camera parameters’ group allows the user to set the number of acquisition frames and integration time. The default image size is set to 32 pixels. As the computation time increases considerably with image size, it is recommended to simulate only a subset of the actual camera field of view.
6. Select ‘Simulate data’ to start the simulation. The simulation will begin by calculating the photons for each handle site of every structure and then converting it to a movie that will be saved as a .raw file, ready for subsequent localization. All simulation settings are saved and can be loaded at a later time with ‘Load from previous simulation’.

? TROUBLESHOOTING

7. (Optional step for multiplexing) Multiplexed Exchange-PAINT data can be simulated by adjusting the ‘Exchange Labels’ setting. For each handle in the custom coordinate system (‘Structure X’, ‘Structure Y’), an Exchange round can be specified. The different imaging rounds can be visually identified by color in the ‘Structure [nm]’ figure. For each round, a new movie file will be generated. By default, the simulation software detects the number of exchange rounds based on the structure definition and will simulate all multiplexing rounds with the same imaging parameters. It is possible to have different imaging parameters for each round, e.g., when using image s with different ON-times. To do so, one can simulate multiplexing rounds individually. In the ‘Exchange rounds to be simulated’ field, enter only the rounds that should be simulated with the current set of parameters. Change the set parameters and the multiplexing round and simulate the next data sets. Repeat until all multiplexing rounds are simulated.

ultra-resolution measurements in this protocol—we did not account for the pixel-dependent noise of our sCMOS camera. Although such calibration might also improve DNA-PAINT image quality, it was not required to achieve the ~1-nm localization precision that allowed us to resolve 5-nm spaced binding sites on DNA origami structures (Fig. 4).

In this protocol, we generally suggest rather long camera integration times (a few hundred milliseconds) as compared with other localization-based microscopy methods such as PALM or STORM. Typically, for localization-based super-resolution techniques, the integration time is roughly matched to the ON-time of blink events to maximize the signal-to-noise ratio of the fluorescence image. Analogously, the integration times suggested here are roughly matched to the binding kinetics of the recommended nine-base-pair DNA duplex. This allows the collection of far more

photons in a single frame as compared with typical PALM or STORM experiments, thus enabling better localization precision. However, it is worth noting that the combination of slower blinking and longer integration time comes at the expense of extended total data acquisition time to detect the same number of events. Nonetheless, it is certainly possible to shorten the binding duration, integration time and thus the total acquisition time by using DNA duplexes with fewer base pairs. For example, the recommended integration time for 8-mers is only tens of milliseconds and that for 7-mers is even less. With such faster kinetics, the integration time and achievable localization precision would then be similar to those in PALM or STORM experiments. An advantage of DNA-PAINT is therefore that it gives the researcher intricate control over the desired localization precision as a trade-off for total acquisition time.

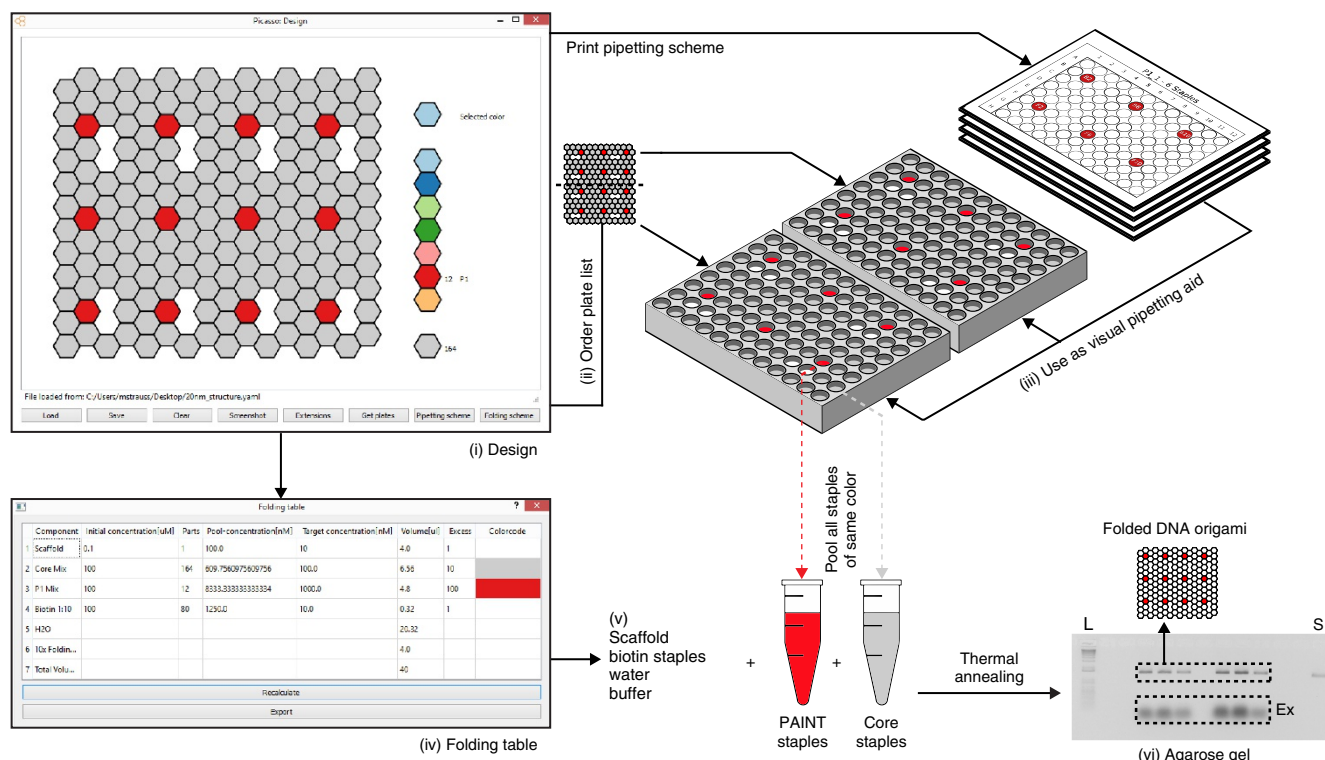


Figure 6 | Designing DNA origami structures for DNA-PAINT with ‘Picasso: Design’. (i) Screenshot of the design interface displaying a 20-nm grid structure with 12 docking sites (red) selected to carry the extension P1. After design is completed, a list of plates is generated as a .csv file ready for ordering (ii). ‘Picasso: Design’ also creates PDF sheets that can be placed underneath the ordered 96-well plates to facilitate pipetting of staple strands (iii). The folding table (iv) gives detailed instructions for preparing components to assemble the DNA nanostructure through thermal annealing. Staple master mixes are pipetted from the plates according to the pipetting scheme. For a successful assembly process, single-stranded DNA scaffold, biotinylated staples, staple master mixes (unmodified core (gray) and docking-strand-extended (red) staples), water and folding buffer need to be mixed (v). After structures are formed (usually through thermal annealing), an agarose gel can be run for analysis or subsequent structure purification (vi). Here, a DNA ladder (L) and the scaffold strand (S) are seen as clear bands together with bands for the correctly folded DNA structures and excess staple strands (Ex). Extracted origami structures are now ready for DNA-PAINT imaging.

The number of localizations and thus the total experiment time strongly influence the resolution of a localization-based super-resolution image. Ideally, to resolve a target structure, it should be spatially probed at least at its Nyquist frequency⁶¹. More precisely, it has been shown that the overall image resolution for localization-based super-resolution microscopy is governed by two main factors: sampling density and localization precision¹⁶. In the same work, it was demonstrated that longer acquisition times increase spatial resolution of the reconstructed image because of increased spatial sampling up to the point at which image resolution is solely limited by localization precision. As the molecule density of a target structure might be unknown, it is often necessary to evaluate a range of acquisition times to determine how many frames are sufficient to represent the structure with the desired resolution. *In silico* simulations of localization-based super-resolution imaging can be a practical method of assaying a large number of data acquisition parameters such as the total acquisition time⁶², reducing the need for time-consuming experiments. The Picasso software package comes with a module for simulating DNA-PAINT data, thus providing the tools for this approach. A more detailed discussion of the ‘Picasso: Simulate’ module follows below. Finally, we want to provide an exemplary thought-experiment as a guide to estimating appropriate acquisition lengths *t*. Consider an imager concentration

c of 10 nM and a probe association rate k_{on} of 10^6 (Ms)⁻¹. This leads to a mean time in between binding events (or dark time τ_d) for a single site of 100 s according to $\tau_d = (k_{on} \times c)^{-1}$. For an ~98% probability (*P*) of any single binding site being visited at least once, a total imaging time of $t = 4 \times \tau_d = 400$ s is required, according to $P = 1 - e^{-t/\tau_d}$. To achieve multiple binding events per site resulting in a decent image quality, we recommend a total imaging time of ~33 min.

In silico simulation of DNA-PAINT data

A fundamental challenge in single-molecule localization microscopy is to systematically design, optimize and validate super-resolution experiments. *In silico* simulations provide a convenient way to address this challenge. Software packages such as SuReSim generate a ground truth model and simulate localization microscopy data using parameters matching an experimental microscope setup⁶². Similar to this approach, the Picasso software suite can simulate localization data with its ‘Simulate’ component, which is specifically tailored to DNA-PAINT. In a graphical user interface, shown in **Figure 7** and **Supplementary Figure 2**, simulation parameters can be set for the type of target structure, DNA-PAINT kinetics, dye properties and hypothetical data acquisition settings such as integration time and total number of acquisition frames.

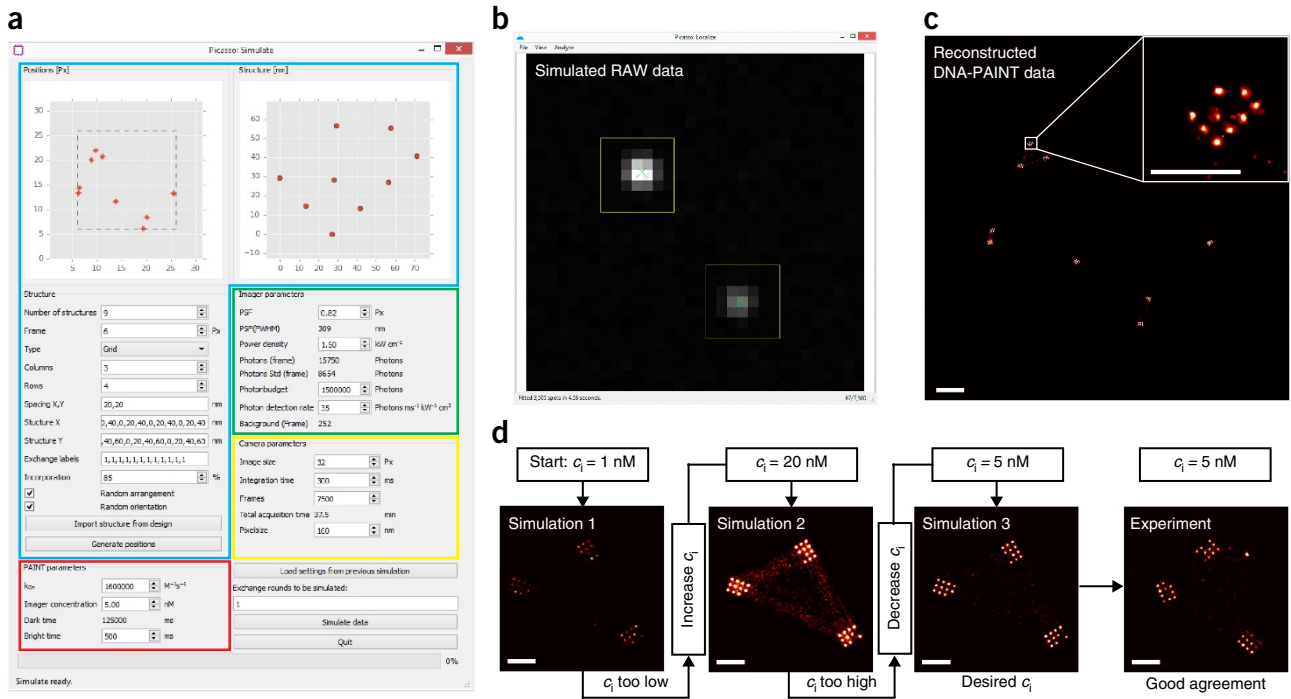


Figure 7 | Simulating DNA-PAINT raw data from DNA origami-like structures. **(a)** Overview of the graphical user interface for ‘Picasso: Simulate’. A DNA-PAINT simulation can be defined by parameters in four categories, indicated by colored frames: ‘Structure’ (blue), PAINT parameters’ (red), ‘Imager parameters’ (green) and ‘Camera parameters’ (yellow). Two overview plots are shown in the upper row. ‘Positions [Px]’ shows the arrangement of individual structures within the field of view and ‘Structure [nm]’ shows the positions of DNA-PAINT binding sites in an individual structure. The positions of binding sites in individual structures can be defined in the ‘Structure’ section by (i) importing RRO structures designed with ‘Picasso: Design’, (ii) using predefined geometric shapes (circles, grids), or (iii) manually entering coordinates. In the ‘PAINT parameters’ section, kinetic parameters for DNA-duplex formation can be set. Imager-related properties (PSF width, laser power, photon budget, photon detection rate and background) are defined in the ‘Imager parameters’ section. Last, acquisition settings, such as image size, integration time, number of frames and pixel size can be set in the ‘Camera parameters’ section. **(b)** Example of simulated raw DNA-PAINT data in ‘Picasso: Localize’ after spot identification and fitting. The simulation program simulates blinking events as if they were acquired with a microscope. **(c)** Reconstructed DNA-PAINT image from data generated with ‘Picasso: Simulate’. The overview of all structures corresponds to the ‘Positions [Px]’ window shown in **a**. A close-up shows the structure that is presented in the ‘Structure [nm]’ window in **a**. **(d)** Example of an iterative process for optimizing DNA-PAINT experiments with simulations. A DNA origami structure is simulated with an imager concentration of 1 nM (Simulation 1). The simulation shows that the concentration is too low, because features of the structure are not clearly visible. Consequently, in a next iteration, data are simulated with a higher concentration, here 20 nM (Simulation 2). Now the simulation reveals that the imager concentration chosen is too high, resulting in ‘cross-talk’ localizations between the structures. Such cross-talk arises when two imagers bind simultaneously to nearby structure sites. Their diffraction-limited images spatially overlap and are falsely identified as a single event with a fitted center coordinate in between the two true positions. For the next iteration, the imager concentration is decreased to 5 nM. The resulting simulation shows structures with clear features and no inter-structure cross-talk. Hence, the 5 nM imager concentration was chosen to perform a DNA-PAINT experiment (Experiment), which in turn is in good agreement with the simulation. Scale bars, 500 nm (**c**), 100 nm (**c** inset, **d**).

The simulated imaging targets are nanometer-sized 2D structures (similar to RROs) on which the positions of DNA-PAINT handles can be defined. These handles serve as a ground truth model for localization events. On the basis of the values set for DNA-PAINT kinetics, the simulation algorithm will calculate a kinetic series of ON- and OFF-events over the total acquisition time for each handle.

The duration of an ON-event is calculated by random selection from an exponential distribution defined by a mean ON-time. This time can be either determined experimentally (i.e., using Picasso’s kinetic analysis tool; see Step 69B) or estimated by the number of base pairs in the imager/docking strand duplex¹⁹. The length of an OFF-event is generated accordingly. Here, the mean OFF-time is calculated from the user-defined binding rate constant and the imager concentration¹⁹.

The user-defined integration time of the simulated camera is used as a sampling window to calculate how long an imager was

bound during each frame. To emulate experimental results, the simulation randomly selects a photon detection rate for each binding event from a normal distribution. The mean and standard deviation of this normal distribution increase linearly with the user-definable laser power density according to experimentally determined coefficients. For each frame (or fraction of a frame) in which the binding event occurs, the detected number of photons is then selected randomly from a Poisson distribution. The mean of this Poisson distribution is equal to the mean expected photon number for the binding event duration within this frame (photon detection rate × duration). In addition, the simulation considers an upper-limit for detected photons from a single binding event, based on a user-defined photon budget per fluorophore.

After the number of photons for all binding events in each frame is calculated, photons are distributed around the center position of their handle by a user-adjustable 2D normal distribution, representing the microscope’s point spread function (PSF).

This results in a list of all photon positions for each frame, which is converted to an image by calculating a 2D histogram. Poissonian noise is added to each frame specified by the background level. Finally, the frames are exported as a raw movie file. The default values for all parameters were estimated from calibration experiments on our TIR fluorescence (TIRF) setup described in the EQUIPMENT section. The imager sequence for calibration experiments was CTAGATGTAT (P1), which was labeled with a Cy3B dye that was excited by a 561-nm laser.

Super-resolution image reconstruction

After a movie of DNA-PAINT data has been acquired (either *in silico*, *in vitro* or *in situ*), single-molecule spots must be identified and fitted to find their center position with subpixel accuracy. These routines are performed with Picasso's 'Localize' component. An overview of the graphical user interface with identified and fitted localizations is shown in **Supplementary Figure 3**, as well as screenshots of parameter dialogs.

A multitude of spot identification algorithms have been developed and applied to localization-based super-resolution microscopy⁶³. In 'Picasso: Localize', spot identification makes use of the image gradient to minimize the impact of nonhomogeneous background. First, local maxima are detected by identifying pixels with highest count in their local neighborhood. This local neighborhood is defined by a square box around the pixel with a user-defined side length. Then, the net gradient (G_{net}) is calculated for each box around a local maximum pixel by

$$G_{net} = \sum_{box} g_i \cdot \mathbf{u}_i$$

where the sum is taken over all pixels of the box, g_i is the central difference gradient at pixel i and \mathbf{u}_i is a unit vector originating at pixel i and pointing toward the center pixel of the box. Hence, the net gradient of a spot is the sum of intensity flowing toward the spot center, which is roughly proportional to the number of signal photons. A user-defined minimum threshold for the net gradient defines whether a spot will be further considered for fitting or disregarded.

After spots have been identified by the net gradient method, their box serves as input for a maximum likelihood fitting procedure⁶⁴. Although a plethora of spot-fitting algorithms have been published and used for localization microscopy⁶³, we chose to implement the maximum likelihood algorithm because it achieves theoretically minimum uncertainty at the Cramer-Rao lower bound with good computational performance. However, it is critical to this fitting algorithm that the camera images be converted correctly to photons, because the algorithm incorporates the Poisson noise statistics inherent to light detection. In 'Picasso: Localize', the user can set the required parameters for converting camera counts to photons. One result of the maximum likelihood fitting is the Cramer-Rao lower bound (CRLB) for each spot. The localization precision is then obtained by calculating the square root of the CRLB.

Finally, super-resolution images are rendered with the 'Picasso: Render' component based on a list of subpixel spot center coordinates (see **Supplementary Fig. 4** for an interface overview). The super-resolution image is a pixel image with arbitrary pixel size, although super-resolution pixels that are too large result in insufficient spatial sampling and a potential loss in resolution. We define the ratio

of super-resolution image pixels to camera pixels as the 'oversampling' parameter. In Picasso, the oversampling can be set either manually or automatically according to how far the user zooms into the image. In the dynamic case, each computer display pixel corresponds to one pixel of the super-resolution image.

Picasso offers several rendering modes for the super-resolution image. The basic option is to use no 'Blur', in which case the super-resolution image is merely a 2D histogram of localization coordinates⁶⁵. The second option is 'One-Pixel-Blur', in which the 2D histogram is convolved with a Gaussian probability density function of volume and standard deviation equal to one. The third option, 'Global Localization Precision', is similar to the 'One-Pixel-Blur'. However, the standard deviation of the Gaussian kernel is set to the median localization precision of all localization coordinates. In the fourth option, 'Individual Localization Precision', each localization is added to the super-resolution image as a Gaussian probability density with volume equal to one and standard deviation equal to the individual coordinate localization precision³. For the localization-precision-based representation methods ('Global' and 'Individual Localization Precision'), a minimum blur width can be defined by the user, so that the blur width is equal to the localization precision, unless the precision is smaller than the set minimum blur width.

Picasso furthermore allows for contrast adjustment of the super-resolution image based on the density of localizations in one super-resolution image—i.e., the number of localizations per pixel (or in the case of 'blurred' images, the sum of probability densities from localizations at each pixel).

Drift correction

A critical post-processing step for localization-based super-resolution imaging is to compensate for stage drift that occurred during data acquisition. In fact, with intricate drift correction methods, extremely high resolution (well below 5 nm) can be achieved²³. After such post-processing steps, drift is almost completely removed as a factor for resolution degradation. Consequently, localization precision and structure sampling are the only remaining factors that determine image quality. Even so, localization precision can be greatly optimized, because DNA-PAINT decouples dye photophysics from blinking, and particle averaging (described below) allows reducing of the effects of undersampling the structure of interest.

Picasso offers two major routes for drift correction: (i) using the localization events themselves and (ii) using specific fiducials in the sample. The localization-events-based drift correction is an implementation of a redundant cross-correlation (RCC) algorithm⁶⁶ in which localizations are split and rendered into multiple super-resolution images according to their temporal appearance in the movie. Image cross-correlation of all resulting super-resolution images then yields the spatial shift between temporal movie segments from which the drift is interpolated. Another conventional way for compensating drift in localization-based super-resolution microscopy is by using fiducial markers³. Such fiducial markers are luminescent and typically observed in the same emission channel as the fluorescent signal. Commonly used fiducials are gold nanoparticles, quantum dots and fluorescently dyed microspheres. With Picasso, localizations from such fiducial markers can be selected and used for drift correction, as the localizations can be assumed to originate from a single

point-like source. Recent developments in extremely high resolution in DNA-PAINT applications have used a large number of DNA origami as fiducial markers²³. When using hundreds of DNA origami structures as markers, their intrinsic size does not affect the drift estimation because of their random rotational orientation. In the same work, an additional drift correction step was applied by selecting single DNA-PAINT binding sites as drift markers. Similar to the case of whole DNA origami, a large number of binding sites (usually several thousands) are required, as each individual site does not comprise sufficient localizations to interpolate the drift for each movie frame accurately. Although DNA origami and their DNA-PAINT binding sites are excellent choices, this type of fiducial-based drift estimation is not limited to these structures. It is feasible to use any distinctly visible landmarks in the image as fiducial markers—for example, protein clusters such as the nuclear pore complex.

In this protocol, we recommend subsequent applications of drift correction by RCC and, if available, fiducial-based correction with DNA origami markers followed by fiducial-based correction with single DNA-PAINT binding sites as markers. Example results after each drift correction step of such a process are shown in **Figure 4b**. In the final images, drift is almost completely eliminated as a factor in image resolution. This is corroborated by the fact that the spread of imaged DNA-PAINT binding sites is similar to the estimated localization precision by nearest neighbor analysis (NeNA)⁶⁷.

Multiplexing

One major benefit of DNA-PAINT is its straightforward extension to multiplexed imaging. Here, the simplest implementation is to use spectrally distinct dyes coupled to orthogonal imager sequences⁶⁸. Unlike other multiplexed localization-based super-resolution techniques⁶⁹, no photo-switching of dyes is necessary, and thus it is rather simple to find compatible spectrally distinct fluorophores⁶⁸ (i.e., Atto488, Cy3B and Atto655).

However, one major drawback of spectral multiplexing is the limited number of distinguishable dyes in the visible spectrum. This limitation can be overcome with Exchange-PAINT²⁰. Here, the unique programmability of DNA-PAINT docking and imager strands is used to enable spectrally unlimited multiplexing by sequentially applying orthogonal imager strands (carrying the same dye) to targets of interest.

In each imaging round, only one imager species is present in solution for one target. After acquisition, the imager is washed out and the imager for the next round is introduced. This is then repeated for the total number of targets. A multicolor image is achieved by assigning a pseudocolor to each imaging round and stacking the acquisitions on top of each other, which is depicted in **Figure 2a**.

Preparation of samples for Exchange-PAINT is similar to that for singleplex experiments, only that an open chamber allowing for fluid exchange is used as displayed in **Figure 2b,c**.

To create multicolor images, Picasso automatically assigns pseudocolors when several data sets are loaded. Different imaging rounds potentially comprise an offset with respect to each other because of instrumentation drift during data acquisition. However, alignment procedures can detect and correct for such image offsets.

Picasso offers cross-correlation or fiducial-based alignment algorithms. When images share features as reference points, such as DNA origami or the general cell shape, the cross-correlation can align images with high precision—e.g., sub-5-nm channel

alignment, as demonstrated in **Figure 2d–f**. When few reference points are available, e.g., for *in situ* imaging of different cell targets, alignment markers or drift fiducials can be added to the sample and used in Picasso's alignment procedure.

A distinct advantage of Exchange-PAINT over spectral multiplexing is that for each imaging round the same dye is used, and thus misalignment and inhomogeneous image warping due to chromatic aberrations are avoided. This allows for very precise channel alignment and makes Exchange-PAINT ideal for colocalization studies to assess spatial proximity and possible molecular interactions. Such results are illustrated in the *in situ* example in **Figure 2g**, in which the morphology of the mitochondrial network and the spatial relationship to microtubules is studied. It shows how mitochondria are embedded in the microtubule network, as described in previous work⁷⁰.

Quantitative imaging with qPAINT

Most super-resolution studies to date harness their exquisite sub-diffraction spatial resolution to address challenges in the biological sciences by structural imaging. However, although still challenging, counting integer numbers of biomolecules when localization precision is insufficient to spatially resolve them can bring further insight into biological systems^{8,71,72}. To achieve this, researchers began using the spatiotemporal information of single-molecule localization microscopy data sets beyond just binning localization events for visualization. The basic concept involves extracting molecule numbers by evaluating the kinetics of the blinking behavior of photoswitchable molecules^{73–75}. Most of these counting techniques use rather complex modeling of the dye photophysics, in some cases combined with spatiotemporal clustering^{72–76}. However, incumbent techniques have certain limitations that prevent them from achieving the highest accuracy and precision over a wide range of molecular densities in resolution-limited areas. These limitations generally lead to overcounting or undercounting artifacts, because the dyes typically have environmentally sensitive photophysics that are hard to predict and model. Furthermore, distinct dyes behave differently even under similar experimental conditions, which severely complicates multiplexed quantitative imaging. In addition, inhomogeneous excitation and photoactivation intensities due to uneven illumination across a sample can lead to inaccurate quantification as well. Last, dyes typically bleach over the course of an experiment, which deteriorates quantification accuracy and precision.

Recently, DNA-PAINT has been used to achieve precise and accurate counting—because of its independence from dye photophysics and immunity to photobleaching—in an implementation called qPAINT²². In contrast to the traditional approach of fixing blinking dyes to the target molecule, DNA-PAINT creates target 'blinking' by transient binding of dye-labeled imager strands to complementary docking strands on the target. As opposed to dye photoswitching, DNA hybridization kinetics is more predictable. Hence, combined with the effective absence of photobleaching, qPAINT can extract molecule numbers with high precision and accuracy.

Figure 3 illustrates the procedure and results of a typical qPAINT experiment. Using Picasso's quantification capabilities, we now provide users with an integrated software solution for calibrating and quantifying molecule numbers in DNA-PAINT data sets. qPAINT relies on the fact that mean dark times for a given influx rate of imager strands ($\xi = k_{\text{on}} \times c$) are dependent

only on the number of docking strands (and thus biomolecules) in an area of interest. To illustrate this, we compare two DNA origami structures, carrying 12 or 42 binding sites in 20-nm and 10-nm grid arrangements, respectively (Fig. 3a). A schematic representation of their respective intensity vs. time traces is shown in Figure 3b. By plotting the cumulative distribution function of both dark time distributions, we can obtain mean dark times for the two structures (Fig. 3c). To translate these dark times to actual numbers of binding sites (or units), the influx rate per unit needs to be calibrated. This can be achieved with DNA origami structures in which binding sites can be visually identified (see Fig. 3d, 20-nm grid structures displaying 12 binding sites). In Picasso, users can now select these calibration structures displaying a known number of units (or binding sites in this case) and calibrate the probe influx rate for subsequent quantification of target molecules of interest in the same data set (Fig. 3d).

The results for a typical qPAINT experiment post calibration are illustrated in Figure 3e–g. 20-nm DNA origami grid structures can be used to compare visually counted numbers of spots with qPAINT results, which are in good agreement (Fig. 3e). Note that not all DNA origami carry all binding sites, because typical staple incorporation efficiencies are <100%. qPAINT allows binding-site identification on 10-nm DNA origami grid structures, in which single sites are not clearly identifiable (Fig. 3f).

Finally, Picasso allows users to quickly obtain statistics from qPAINT data sets using its integrated ‘Pick’ and ‘Pick similar’ tools. Figure 3g illustrates the resulting number of binding-site distributions for 20-nm and 10-nm DNA origami grid structures in a single sample. The average number of binding sites is in excellent agreement with expectations. For 20-nm structures, the incorporation efficiency is ~78%, whereas it is slightly lower for 10-nm grid structures at 70%. This, however, is to be expected, as staple incorporation efficiency should be lower for larger numbers of modified staple strands in DNA origami structures.

Filtering localizations

After identification and fitting of single-molecule spots, filtering the list of localizations might improve super-resolution image quality^{3,5,6,69,70,77}. Only after fitting a single-molecule spot, are properties such as spot width or an accurate estimation of the number of photons available. Hence, spot identification itself may not reliably rule out false-spot detections. A typical filtering procedure is to remove localizations with spot widths that are too small or too large. Ideally the spot width matches that of the microscope’s PSF. Therefore, if the spot width is, for example, too big, it is likely that the spot originates from two closely and overlapping events. The resulting fit coordinate will be between the two correct center positions and should therefore be disregarded. Another example of filtering is to remove localizations with a number of photons or a localization precision that is too low. After such filtering, the super-resolution image quality can improve, because only high-precision localizations remain. Picasso’s ‘Filter’ component provides a convenient, visually guided way to filter localizations based on histograms of their properties. An overview of its graphical user interface, as well as screenshots of filtering procedures in progress, is shown in Supplementary Figure 5. We recommend studying histograms of localization properties and joint histogram maps of two localization properties with the goal of identifying the true signal

population and removing false populations or outliers. An overview of localization properties saved by Picasso is shown in the **Supplementary Manual**.

Particle averaging

When imaging a structure that appears multiple times in the field of view, aligning the individual images on top of each other and ‘summing them up’ can generate an ‘average’ image with improved image quality^{23,78}. Such a procedure is analogous to the particle averaging often applied for structural biology in single-particle electron microscopy⁷⁹ and has already been successfully applied to localization-based super-resolution microscopy^{80,81}. Although, strictly speaking, we do not create an ‘averaged’ but rather a ‘sum image’ from all localizations, we here will continue to use the notion of averaging as a historical term from the electron microscopy field. ‘Averaging’ primarily increases the image signal-to-noise ratio, which translates for localization microscopy to the proportion of true, high-precision localizations (signal) to false or imprecise localizations (noise). Hence, structure sampling, a major factor for image resolution¹⁶, can be improved by the averaging procedure. This is exemplified by the individual and average images of two RRO DNA origami structures in Figure 4c–f, showing the letters ‘MPI’ and ‘LMU’. The average image comprises a greatly enhanced signal-to-noise ratio as compared with images of individual structures. Moreover, even though some binding sites are missing in individual structures, averaging could reconstruct all binding sites and resolve their ~5-nm distances well.

Picasso offers a graphical user interface for averaging multiple images of the same structure with the ‘Average’ component. The underlying algorithm does not require a reference and is based on a traditional procedure borrowed from single-particle electron microscopy⁸². Briefly, the individual images are first translationally aligned on top of each other by overlaying the center of mass of localizations. Then, several iterations of rotational and refined translational alignment are applied. In each iteration, an average image is constructed by pooling all localizations and rendering them on a super-resolution pixel grid. Then, localizations from each individual structure are rotated over 360 degrees in small steps and rendered as a super-resolution image for each rotational step. The angular step size is dynamically chosen so that the rotation distance at twice the root mean square (RMS) deviation of all localizations from their center of mass matches the size of a super-resolution pixel. Each rotated image is cross-correlated with the average image of the current iteration, and the maximum value and position of the cross-correlation are recorded. Finally, the localizations of an individual structure are rotated and translated according to the rotation and translation with the highest cross-correlation value. In the next iteration, a new improved average image can be generated from the now updated localization coordinates. After a certain number of iterations, the average image will converge—i.e., the pixel values will not change after an iteration. At this point, the algorithm can be stopped, and the new localization list is saved.

Averaging results, as shown in Figure 4e,f, rely on experimental conditions and post-processing steps that are specifically aimed at ultra-resolution. In particular, intricate drift correction as described above is a key contribution. Experimental conditions for ultra-resolution are described in **Box 2**; refer to **Supplementary Figures 6–9** for structure design.

MATERIALS

REAGENTS

! CAUTION All reagents can be potentially hazardous and should be handled only by trained personnel.

DNA labeling

- PBS, pH 7.2 (Life Technologies, cat. no. 20012-019)
- 0.5 M EDTA, pH 8.0 (Ambion, cat. no. AM9261) **! CAUTION** EDTA may cause eye and skin irritation; avoid breathing the dust or fumes.
- DMF (Thermo Fisher Scientific, cat. no. 20673) **! CAUTION** DMF is a toxic and flammable liquid; protect your eyes and skin, and avoid breathing the dust or fumes. It may also damage fertility and cause harm to the unborn child. Handle it under a chemical hood.
- AffiniPure Donkey Anti-Rat IgG (Jackson ImmunoResearch, cat. no. 712-005-150)
- AffiniPure Donkey Anti-Rabbit IgG (Jackson ImmunoResearch, cat. no. 711-005-152)
- AffiniPure Goat Anti-Mouse IgG (Jackson ImmunoResearch, cat. no. 115-005-003)

Antibody labeling via maleimide-PEG2-succinimidyl ester

- Maleimide-PEG2-succinimidyl ester (Sigma-Aldrich, cat. no. 746223)
- No-Weigh Format DTT (Thermo Fisher Scientific, cat. no. 20291)
- ! CAUTION** This compound causes skin and respiratory pathway irritation, as well as serious eye irritation. It is toxic if swallowed and causes long-term damage to aquatic life.

- Micro BCA Protein Assay Kit (Thermo Fisher Scientific, cat. no. 23235)

- Thiol-DNA (P1 handle: Thiol-TTATACATCTA; MWG Eurofins)
- Thiol-DNA (P3 handle: Thiol-TTCTTCATTA; MWG Eurofins)

Antibody labeling via DBCO-sulfo-NHS ester

- DBCO-sulfo-NHS ester (Jena Bioscience, cat. no. CLK-A124-10)
- Azide-DNA (Biomers.net) P1 Handle: Azide-TTATACATCTA
- Azide-DNA (Biomers.net) P3 Handle: Azide-TTCTTCATTA

Immunofixation and cell imaging

- 8-well chambered cover glasses (Eppendorf, cat. no. 0030742036 or Thermo Fisher Scientific, cat. no. 155409)
- BSA (Sigma-Aldrich, cat. no. A4503-10g)
- Triton X-100 (Carl Roth, cat. no. 6683.1) **! CAUTION** This compound is toxic if swallowed, and it can cause serious eye damage.
- 0.22- μ m sterile filters (Merck/EMD Millipore, cat. no. SLGS033SS)
- Sodium chloride (Ambion, cat. no. AM9759) **! CAUTION** Sodium chloride may cause skin and eye irritation, and it may be harmful if inhaled or swallowed.
- Sodium borohydride (Carl Roth, cat. no. 4051.1) **! CAUTION** This compound reacts in a volatile manner with H₂O, is toxic if swallowed and can cause serious skin damage. Handle it under a chemical hood.
- 16% (vol/vol) Paraformaldehyde (Electron Microscopy Sciences, cat. no. 15710) **! CAUTION** This compound is flammable, a carcinogen and toxic if swallowed; avoid breathing the fumes or dust. It can cause serious eye, skin or respiratory pathway irritation. Handle it under a chemical hood.
- 25% (vol/vol) Glutaraldehyde (SERVA, cat. no. 23115.01) **! CAUTION** Glutaraldehyde is toxic if swallowed; it causes serious skin damage, and acute and chronic toxicity in aquatic life. Avoid breathing the fumes or dust. Wear protective equipment and handle the compound under a chemical hood.
- α -Tubulin (YL1/2) antibody (Thermo Fisher Scientific, cat. no. MA1-80017)
- α -Tubulin (DM1A) mouse antibody (Cell Signaling, cat. no. 3873S)
- Tom20 (FL-145) rabbit antibody (Santa Cruz, cat. no. sc-11415)
- DNA-labeled secondary antibodies and imager kit (Ultravue, cat. no. U10001)
- Imager strand (P1-Cy3B: CTAGATGTAT-Cy3B; Eurofins Genomics)
- Imager strand (P3-Atto655: GTAATGAAGA-Atto655; Eurofins Genomics)
- Imager strand (P3-Cy3B: GTAATGAAGA-Cy3B; Eurofins Genomics)

Cell culture

- PBS, pH 7.2 (Thermo Fisher Scientific, cat. no. 20012-019)
- MEM (Thermo Fisher Scientific, cat. no. 31095-052)
- Eagle's Minimum Essential Medium (EMEM; ATCC, cat. no. 30-2003)
- L-Glutamine (Thermo Fisher Scientific, cat. no. 25030-149)
- Non-essential amino acids (Thermo Fisher Scientific, cat. no. 11140-035)
- FBS (Thermo Fisher Scientific, cat. no. 10500-064)
- Penicillin-streptomycin (P/S; Thermo Fisher Scientific, cat. no. 15140-122)
- ! CAUTION** It may damage fertility and cause harm to the unborn child. Avoid breathing fumes or dust.
- Trypsin-EDTA (Thermo Fisher Scientific, cat. no. 25300-054)

- HELA cell line (Leibniz Institute DSMZ: Catalogue of Human and Animal Cell Lines (<http://www.dsmz.de>), cat. no. ACC-57) **! CAUTION** The cell lines used in your research should be regularly checked to ensure that they are authentic and they are not infected with mycoplasma.

- BS-C-1 cell line (ATCC, cat. no. CCL-26) **! CAUTION** The cell lines used in your research should be regularly checked to ensure that they are authentic and they are not infected with mycoplasma.

DNA origami folding

- Staple strands, modified and unmodified (Eurofins Genomics)
- M13 bacteriophage ssDNA scaffold p7249 (New England BioLabs, cat. no. N4040S)
- Tris, pH 8.0, 1 M (Ambion, cat. no. AM9856) **! CAUTION** Tris can cause skin and serious eye irritation.
- EDTA, pH 8.0, 0.5 M (Ambion, cat. no. AM9261) **! CAUTION** EDTA may cause eye and skin irritation; avoid breathing the dust or fumes.
- Water (Gibco, cat. no. 10977-035)
- Magnesium, 1 M (Ambion, cat. no. AM9530G)
- Agarose (Biomol, cat. no. 01280.100)
- 50 \times TAE Buffer (Fluka Analytical, cat. no. 67996-10L-F)
- SYBR safe DNA gel stain (Invitrogen, cat. no. SS33102) **! CAUTION** Protect your eyes and avoid breathing the dust, fumes or mist; it causes eye, skin and respiratory irritation.
- DNA gel loading dye (Thermo Fisher Scientific, cat. no. R0611)
- DNA ladder (Invitrogen, cat. no. 10787-018)

In vitro sample preparation

- Protocatechuic acid (PCA; Sigma-Aldrich, cat. no. 37580-25G-F) **! CAUTION** PCA causes skin, respiratory pathway and serious eye irritation. Avoid breathing the dust, fumes or mist.
- Protocatechuate 3,4-dioxygenase (PCD; Sigma-Aldrich, cat. no. P8279-25UN)
- Trolox (Sigma-Aldrich, cat. no. 238813-1G) **! CAUTION** Trolox causes skin, respiratory pathway and serious eye irritation. Avoid breathing the dust, fumes or mist.
- NaOH (VWR, cat. no. 31627.290) **! CAUTION** NaOH causes serious skin and eye damage; avoid breathing the dust, fumes or mist. Wear protective equipment.
- Methanol (Sigma-Aldrich, cat. no. 32213-2.5L) **! CAUTION** Methanol is a flammable liquid, and it is toxic upon ingestion and skin contact; avoid breathing the dust, fumes or mist.
- Potassium chloride (Carl Roth, cat. no. 6781.1)
- Glycerol (Sigma-Aldrich, cat. no. 65516-500ml)
- Isopropanol (Carl Roth, cat. no. 33539-2.5L-R) **! CAUTION** Vapor and liquid phases are easily flammable, and the compound causes heavy eye irritation.
- Epoxy Glue (Toolcraft, cat. no. TC-EPO5-24)
- Albumin, biotin-labeled bovine (Sigma-Aldrich, cat. no. A8549-10MG)
- Streptavidin (Thermo Fisher Scientific, cat. no. S888)
- Tween 20 (Sigma-Aldrich, cat. no. p2287)

EQUIPMENT

- Thermocycler (Mastercycler Nexus Gradient; Eppendorf, cat. no. 6331000017)
- 10-liter Tank (Carl Roth, cat. no. K653.1)
- Sub-cell GT system gel chamber (Bio-Rad, cat. nos. 170 4401-4406 and 170 4481-4486)
- PowerPac basic power supply (Bio-Rad, cat. no. 1645050)
- Microwave (Severin, cat. no. 7891)
- Erlenmeyer flask, 250 ml (Carl Roth, cat. no. NY87.1)
- Razor blade (Carl Roth, cat. no. CK07.1)
- Visi-blue light transilluminator (UVP, cat. no. 95-0461-02)
- Centrifuge 5430R (Eppendorf, cat. no. 5428000414)
- NanoDrop 2000c (Thermo Fisher Scientific, cat. no. ND-2000c)
- Shaker (GFL, cat. no. 3015)
- Biological safety cabinet (HeraSafe; Thermo Electron Corporation, cat. no. 51022482)
- Water purification system (PURELAB classic; ELGA LabWater, cat. no. CLXXUVFM2)
- Incubator (Heracell 240; Thermo Fisher Scientific, cat. no. 51026333)
- Pipetboy acu 2 (Integra, cat. no. 155017)
- Eppendorf Research plus 0.1–2.5 μ l pipette (Eppendorf, cat. no. 3120000011)
- Eppendorf Research plus 0.5–10 μ l pipette (Eppendorf, cat. no. 3120000020)
- Eppendorf Research plus 2–20 μ l pipette (Eppendorf, cat. no. 3120000038)
- Eppendorf Research plus 10–100 μ l pipette (Eppendorf, cat. no. 3120000046)

- Eppendorf Research plus 20–200 µl pipette (Eppendorf, cat. no. 3120000054)
- Eppendorf Research plus 100–1000 µl pipette (Eppendorf, cat. no. 3120000062)
- Multipette M4 pipette (Eppendorf, cat. no. 4982000314)
- Eppendorf Research plus, 8-channel, 0.5–10 µl pipette (Eppendorf, cat. no. 3122000019)
- Gel imager (Typhoon FLA 9500; GE, cat. no. 28996943)
- Side cutter (Hoffmann Group, cat. no. 725310)
- Amicon spin filters, 3 kDa (Merck/EMD Millipore, cat. no. UFC500396)
- Amicon spin filters, 100 kDa (Merck/EMD Millipore, cat. no. UFC510096)
- Nap5 columns (GE Healthcare, cat. no. 17-0853-02)
- Zeba desalting spin columns (Thermo Fisher Scientific, cat. no. 89882)
- Amicon spin filters, 100 kDa (Merck/EMD Millipore, cat. no. UFC510096)
- NORM-JECT 2-ml syringe (Henke Sass Wolf, cat. no. 4020-000V0)
- NORM-JECT 10-ml syringe (Henke Sass Wolf, cat. no. 4100-000V0)
- NORM-JECT 20-ml syringe (Henke Sass Wolf, cat. no. 4200-000V0)
- FINE-JECT Needle, 1.2 × 40 mm (Henke Sass Wolf, cat. no. 4710012040)
- FINE-JECT Needle, 1.1 × 40 mm (Henke Sass Wolf, cat. no. 4710011040)
- Silicon tubing, inner diameter = 0.5 mm, outer diameter = 1 mm (GM GmbH, cat. no. 35605)
- T75 Flasks (Falcon, cat. no. 353136)
- 10-ml Serological pipettes (Greiner Bio-One, cat. no. 607180)
- 5-ml Serological pipettes (Greiner Bio-One, cat. no. 606180)
- 2-ml Serological pipettes (Falcon, cat. no. 357507)
- Glass Pasteur pipettes (Brand, cat. no. 747720)
- 90-nm Gold particles (prepared in house⁸³)
- DNA LoBind Tube, 0.5 ml (Eppendorf, cat. no. 0030 108.035)
- PCR tubes (Trefflab, cat. no. 96.09852.9.01)
- Freeze 'N Squeeze columns (Bio-Rad, cat. no. 732-6165)
- Aluminum foil (VWR, cat. no. 391-1257)
- 1.5-ml Eppendorf tubes (Eppendorf, cat. no. 0030 120.086)
- 15-ml Falcon tubes (Falcon, cat. no. 352096)
- 50-ml Falcon tubes (Falcon, cat. no. 352070)
- ibidi sticky-Slide VI 0.4 (ibidi, cat. no. 80608)
- High-precision cover glasses 18 × 18 mm, no. 1.5H (Marienfeld, cat. no. 0107032)
- High-precision cover glasses 24 × 60 mm, no. 1.5H (Marienfeld, cat. no. 0107242)
- Microscopy slide (Thermo Fisher Scientific, cat. no. 10756991)
- Double-sided adhesive tape (Scotch, cat. no. 665D)
- Weighing paper (VWR International, cat. no. 12578-121)

TIRF super-resolution setup

- Optical air table (Newport, cat. no. RS4000-46-12)
- Inverted fluorescence microscope (Nikon, Ti Eclipse with Perfect Focus System)
- XY Stage (Physik Instrumente, cat. no. M-545.2MN)
- Lenses and mirrors (Thorlabs)
- Filter cubes (Chroma Technology, cat. nos. TRF49904-NK, TRF49909-NK, TRF49914-NK)
- Oil-immersion objective, 100× Apo SR TIRF objective, numerical aperture (NA) = 1.49, working distance (WD) = 0.12 (Nikon)
- Immersion oil, refractive index (*n*) = 1.515 (23 °C), (Nikon, Type A)
- sCMOS camera (Hamamatsu Orca Flash 4.0 V2)
- EMCCD camera (Andor, iXon Ultra, model no. DU-897)
- Excitation laser, 488 nm, 200 mW (Toptica iBeam smart, model no. 488-S-HP)
- Excitation laser, 561 nm, 200 mW (Coherent Sapphire, model no. 561-200 CW CDRH)
- Excitation laser, 640 nm, 150 mW (Toptica, iBeam smart, model no. 640-S)
- Microscopy slide thermal power sensor (Thorlabs, model no. S170C)
- Digital power meter (Thorlabs, model no. PM100D)
- Acquisition computer: a computer used to acquire microscope data with the µManager software package⁵⁸. See EQUIPMENT SETUP for hardware requirements.
- Analysis computer: a computer with a Microsoft Windows 64-bit operating system. See EQUIPMENT SETUP for hardware requirements.
- Analysis software: our analysis software package 'Picasso' can be downloaded from our website at <http://www.jungmannlab.org>.

REAGENT SETUP

Pre-extraction buffer The pre-extraction buffer consists of 0.4% (vol/vol) glutaraldehyde and 0.25% (vol/vol) Triton X-100 in 1× PBS at pH 7.2. It can be stored at –20 °C for 12 months.

Enhanced microtubule fixative The enhanced microtubule fixative consists

of 3% (vol/vol) glutaraldehyde in 1× PBS at pH 7.2, and it can be stored at –20 °C for 12 months.

Standard fixative The standard fixative consists of 3% (vol/vol) paraformaldehyde and 0.1% (vol/vol) glutaraldehyde in 1× PBS at pH 7.2. It can be stored at –20 °C for 12 months.

Blocking solution The blocking solution contains 3% (wt/vol) BSA and 0.2% (vol/vol) Triton X-100 in 1× PBS at pH 7.2, and it must be filter-sterilized. It can be stored at 4 °C for up to 6 weeks.

Antibody dilution solution The antibody dilution solution contains 3% (wt/vol) BSA in 1× PBS at pH 7.2, and it must be filter-sterilized. It can be stored at 4 °C for up to 6 weeks.

DTT solution The DTT solution consists of 250 mM DTT, 1.5 mM EDTA and 0.5× PBS, pH 7.2. It must be freshly prepared for the reduction of the thiolated DNA.

BCA mix The BCA mix includes 500 µl of reagent A, 500 µl of reagent B and 25 µl of reagent C (from the Micro BCA Protein Assay Kit), and it must be freshly prepared.

HeLa cell medium The HeLa cell medium consists of MEM, 10% (vol/vol) FCS, 1% (vol/vol) P/S, 2 mM L-glutamine and 1× non-essential amino acids. HeLa cell medium can be stored at 4 °C for up to 4 months.

BSC1 cell medium The BSC1 cell medium consists of EMEM, 10% (vol/vol) FCS and 1% (vol/vol) P/S.

Cross-linker aliquots Cross-linkers should be divided into aliquots at a concentration of 10 mg/ml in DMF, and they can be stored at –80 °C for up to 12 months.

Buffer A Buffer A consists of 10 mM Tris-HCl and 100 mM NaCl at pH 8.0, and it can be stored at room temperature (RT; 21 °C) for 6 months.

Buffer A+ Buffer A+ consists of 10 mM Tris-HCl, 100 mM NaCl and 0.05% (vol/vol) Tween 20 at pH 8.0, and it can be stored at RT for 6 months.

Buffer B Buffer B consists of 5 mM Tris-HCl, 10 mM MgCl₂ and 1 mM EDTA at pH 8.0, and it can be stored at RT for 6 months.

Buffer B+ Buffer B+ consists of 5 mM Tris-HCl, 10 mM MgCl₂, 1 mM EDTA and 0.05% (vol/vol) Tween 20 at pH 8.0, and it can be stored at RT for 6 months.

Buffer C Buffer C consists of 1× PBS at pH 7.2 supplemented with additional 500 mM NaCl, and it can be stored at RT for up to 6 months.

Exchange washing buffer Exchange washing buffer consists of Buffer B+ for *in vitro* samples and of 1× PBS, pH 7.2, for *in situ* samples; it can be stored at RT for 6 months.

100× Trolox solution 100× Trolox solution consists of 100 mg of Trolox, 430 µl of methanol and 345 µl of NaOH (1 M) in 3.2 ml of H₂O. It should be divided into 20-µl portions in PCR tubes and can be stored at –20 °C for up to 6 months.

40× PCA solution 40× PCA solution consists of 154 mg of PCA in 10 ml of water, adjusted to pH 9.0 with NaOH. The solution should be divided into 20-µl aliquots in PCR tubes and can be stored at –20 °C for up to 6 months.

100× PCD solution 100× PCD solution consists of 9.3 mg of PCD and 13.3 ml of buffer (50% glycerol stock in 50 mM KCl, 1 mM EDTA and 100 mM Tris-HCl, pH 8.0). It should be divided into 20-µl aliquots in PCR tubes and can be stored at –20 °C for up to 6 months.

Oxygen-scavenging system PPT solution PPT solution consists of a 1:1:1 ratio of 1× PCA/1× PCD/1× Trolox. Mix with imaging buffer at least 1 h before imaging.

Imager solution For *in vitro* samples, the imager solution consists of 1× Buffer B+, optional scavenger system PPT solution (1× Buffer B+, 1× PCA, 1× PCD, 1× Trolox) and a fluorophore-labeled DNA strand. For *in situ* samples, the imager solution consists of 1× Buffer C, optional scavenger system PPT solution (1× Buffer C, 1× PCA, 1× PCD, 1× Trolox) and a fluorophore-labeled DNA strand. The concentration range for the fluorophore-labeled DNA strand is highly target dependent, but it ranges between 100 pM and 10 nM. The solution should always be freshly prepared.

10× Folding buffer 10× folding buffer consists of 125 mM MgCl₂, 100 mM Tris and 10 mM EDTA at pH 8.0, and it can be stored at RT for up to 6 months.

Gel buffer Gel buffer consists of 1× TAE buffer, and it can be stored at RT for 1 year.

Gel running buffer Gel running buffer consists of 1× TAE buffer and 12.5 mM MgCl₂, and it can be stored at RT for up to 1 year.

BSA–biotin stock BSA–biotin stock contains 10 mg/ml BSA–biotin in Buffer A, and it should be divided into 20-µl aliquots. It can be stored at –20 °C for up to 6 months.

PROTOCOL

BSA–biotin solution BSA–biotin solution contains 1 mg/ml BSA–biotin in Buffer A+ and should be freshly prepared. It can be stored for up to 3 d at 4 °C.

Streptavidin stock Streptavidin stock contains 10 mg/ml streptavidin in Buffer A and should be divided into 10- μ l aliquots. It can be stored at –20 °C for up to 6 months.

Streptavidin solution Streptavidin solution contains 0.5 mg/ml streptavidin in Buffer A+ and should be freshly prepared. It can be stored for up to 3 d at 4 °C.

Staple strands Staple strands can be ordered in different purity grades. High-purity salt-free purification is sufficient for standard staples; however, we recommended ordering modified staples, such as those with fluorophores or biotins, HPLC or PAGE purified. Staple strands for nanostructures should be ordered in 96-well plates (0.2 ml) to facilitate the handling and creation of master mixes with the help of multipipettes. To keep the manual handling to a minimum, the staples should be ordered prediluted at a concentration of 100 μ M in H₂O. The plates can be stored at –20 °C for at least 12 months.

EQUIPMENT SETUP

Acquisition computer The following computer system was used for all data acquisition in this protocol: Dell Precision T7910, Dual Intel Xeon Processor E5-2620 v3 at 2.4 GHz (12 cores), 32 GB RAM, four 2 TB HDD configured in a Hardware RAID 0, Windows 7 Professional 64-bit operating system. **▲ CRITICAL** A RAID 0 setup is optimized for fast input/output. For long-term data storage, users are advised to use data storage facilities with daily backup available to research groups at universities or research institutes.

Acquisition software As image acquisition software, install μ Manager, an open-source software⁵⁸ that can be downloaded from <https://micro-manager.org>. Follow the installation instructions and set up the software to control the microscope equipment.

Analysis computer We do recommend performing all postacquisition steps with Picasso on a separate analysis workstation. The hardware requirements depend on the specific file size of the data set to be analyzed. Generally, the most important factors are the number of available CPU cores and RAM. The following system was used for all analyses in this protocol: Dell Precision T7910, Dual Intel Xeon CPU E5-2680 v3 at 2.5 GHz (24 cores), 256 GB RAM and four 2 TB HDD configured in a Hardware RAID 0, Windows Server 2012 R2 64-bit operating system. **▲ CRITICAL** A RAID 0 setup is optimized for fast input/output. For long-term data storage, users are advised to use data storage facilities with daily backup available to research groups at universities or research institutes.

Analysis software Download the ‘Picasso’ installer available at our website (<http://www.jungmannlab.org>). Follow the installation instructions. Multiple Picasso components will appear as shortcuts in a start menu subfolder named ‘Picasso’.

Power density calibration Determine the laser power at the sample by placing the microscopy slide thermal power sensor with immersion oil on the sample holder. The power density is then calculated as an average density over the illuminated area. See **Supplementary Table 1** for an exemplary calibration on our microscope.

Fluid exchange chamber To prepare a fluid exchange chamber for *in situ* imaging, see **Box 1**.

PROCEDURE

Design of DNA nanostructures ● TIMING 1 h

- 1| Start ‘Picasso: Design’, which displays a canvas of a hexagonal lattice, representing the staple strand positions (**Fig. 6**) in a 2D RRO³³.
- 2| Design a pattern of DNA-PAINT binding sites by clicking on the canvas hexagons. Clicking on a hexagon will change its color and marks the respective staple to be extended with an external sequence. Each color corresponds to a specific extension that may be defined later. The default state without an external extension is indicated by a gray hexagon. The center-to-center distance between two hexagons is ~5 nm on the DNA origami. To change the ‘current color’, click on a colored hexagon in the color palette to the right. Clicking on a hexagon with a currently selected color will reset the ‘current color’ to the unmarked state (gray). Click ‘Clear’ to reset all hexagons in the lattice. The eight white double-hexagons within the structure are placeholders for biotinylated staples for surface attachment and are not intended for modification. In total, the structure consists of 176 staples available for modification.
- 3| Click ‘Save’ to save the design. Progress can be saved at any time and loaded at a later point by selecting ‘Load’. A screenshot of the design can be saved by clicking on ‘Screenshot’.
- 4| Click on ‘Extensions’ to specify the extensions corresponding to each color. A table with all the colors present in the design will open. A selection of commonly used DNA-PAINT handles can be obtained via the dropdown menu in the ‘Preselection’ column. This list can be extended by modifying ‘paint_sequences.csv’ in the subfolder ‘picasso’ of the Picasso install directory. See **Supplementary Table 2** for a table of the default sequences. Alternatively, define a custom ‘Shortname’ and ‘Extension’ by entering them in the table. After defining all colors used in the canvas, select ‘OK’ to confirm the extensions. The display will update with the ‘Shortname’. The sequence specified will be added to the 3’-end of the staple and will point out of the structure (away from the cover glass). For a full list of all unmodified core staples, refer to **Supplementary Table 3**.
- 5| Once the design step is complete, the sequences for the corresponding structure need to be obtained. Click on ‘Get plates’ to generate a staple list for ordering. As an RRO origami structure consists of 184 staples, the staples in the list are arranged in two 96-well plates, so that each well corresponds to a position on the hexagonal lattice. It is possible to export only the sequences of a particular structure (in total, two plates) or to get a list of plates for which all possible positions are extended with all extensions used in the design. This is particularly useful in the case in which different origami designs with different extensions and patterns will be tested, so all staples are ready to be mixed and matched for subsequent design iterations. The software will export the list in .csv format, so that the file can be used for direct ordering at your favorite oligo synthesis company. Choose high-purity salt-free purification and order oligonucleotides in solution with a

concentration of 100 μM in H_2O (see also Reagent Setup). Store the .csv file in a folder so that the program can later create pipetting schemes based on your plate stock. In addition, order the biotinylated staples (for cover glass attachment of the DNA origami) that can be found in **Supplementary Table 4**.

■ **PAUSE POINT** Typically, synthesis of unmodified oligonucleotides at a commercial vendor will take between 2 and 10 working days.

Folding of DNA structures ● **TIMING 6–7 h**

6| Once all sequences are obtained, staples with the same extension are pooled together from plates and place in microcentrifuge tubes as stock mixes. Picasso will generate a visual pipetting aid to help identify which staples need to be pooled together in a separate microcentrifuge tube. To so initiate this, select ‘Pipetting scheme’ and select the folder with all previously generated plates. ‘Picasso: Design’ will search in all .csv files in that folder for sequences that are needed for the design. Note that only .csv files that contain staple lists (that were generated with ‘Get plates’ in ‘Picasso: Design’) should be present in that folder. A list will be generated with all necessary sequences and the visual pipetting aid in .pdf format for the origami stock mixes. The dimensions of the printed pipetting scheme match those of typical 96-well plates, so that wells that need to be pipetted can be easily identified.

▲ **CRITICAL STEP** If the software does not find all sequences that are needed in the plate list, it will display an error message but still compile the pipetting aid and the staple list. Missing staples are indicated by ‘NOT FOUND’ in the list.

7| Print out the pipetting aid and place a transparent 96-well plate above it. Pool staples according to their color and the pipetting aid for stock mixes in microcentrifuge tubes. The volume of each staple that is needed when pooling can be estimated considering the final amount of structures. When folding, i.e., 40 μl of DNA origami with a 10-nM final scaffold concentration (enough for ~80 DNA-PAINT experiments), the amount of staples needed is ~0.04 μl for each core staple and ~0.4 μl for each extended staple. As pipetting precision decreases with small volumes, pipette at least 1 μl per staple when pooling for mixes. Avoid contamination of the plates, do not talk while pipetting and cover the plates whenever possible. Seal the plates immediately after use. Store mixes at $-20\text{ }^\circ\text{C}$ in tubes for up to 12 months.

8| Select ‘Folding Scheme’ to generate a table with a folding protocol. Adjust the initial concentrations in the table according to the ordered stocks and click ‘Recalculate’, if applicable. The software will automatically calculate the concentration of a strand in a staple mix depending on the number of staples in the mix. Adjust ‘Excess’ or ‘Total Volume’ to your needs and mix all items on the folding scheme list in the calculated quantities. Refer to **Supplementary Table 5** for n exemplar folding table.

9| Use a thermocycler and fold the origami mix using the following thermal gradient:

Cycle number	Parameters
1	80 $^\circ\text{C}$
2–57	60 $^\circ\text{C}$ –4 $^\circ\text{C}$, 3 min 12 s per $^\circ\text{C}$
58	Hold at 4 $^\circ\text{C}$

■ **PAUSE POINT** The structures can be stored at 4 $^\circ\text{C}$ for up to 1 week or at $-20\text{ }^\circ\text{C}$ in DNA LoBind Tubes for long-term storage (at least several months).

Purification of DNA nanostructures ● **TIMING ~3.5 h**

10| Purify the DNA nanostructures using your favorite method. Several methods for purification of DNA nanostructures, such as Gel⁴², rate-zonal centrifugation⁴³ and PEG⁴⁴, are described in the literature. For DNA-PAINT, it is possible in most cases to use the structures without purification, as excess staple strands will be washed out of the flow chamber.

▲ **CRITICAL STEP** When folding DNA origami for the first time, it is recommended to run an agarose gel to confirm the folding (**Fig. 6**). Typically, well-folded monomeric structures will appear as a single sharp gel band (upper highlighted area in the gel in **Fig. 6**) together with a faster migrating band consisting of excess staple strands (lower highlighted area in the gel in **Fig. 6**).

■ **PAUSE POINT** The structures can be stored at 4 $^\circ\text{C}$ for up to 1 week or at $-20\text{ }^\circ\text{C}$ in DNA LoBind Tubes for at least 1 year.

11| Prepare a solution of 1.8 g of agarose in 120 ml of gel buffer in an Erlenmeyer flask (1.5% (wt/vol)).

PROTOCOL

- 12| Use a microwave to heat up and completely solubilize the agarose solution by stirring the flask in between the heating phases.
! CAUTION Use heat-resistant gloves when handling the hot flask to avoid burns.
- 13| If no agarose particle traces are visible anymore, let the solution cool for 1 min, and add 1.5 ml of 1M MgCl₂ and 14 μl of Sybr Safe.
! CAUTION Avoid inhaling solutions with Sybr Safe.
- 14| Pour the solution into a gel chamber, add an appropriate comb and let it solidify for 45 min.
- 15| Load the gel with the DNA origami structures. Prepare two lanes for a DNA ladder and scaffold (same concentration as origami) as reference. Mix the origami solution with loading dye (20 μl of folded DNA Origami + 5 μl of loading dye) and run the gel in running buffer at 90 V for 90 min at 4 °C or on ice.
- 16| Acquire an image using a gel imager for documentation.
- 17| Cut out the origami band with a razor blade on a blue-light transilluminator table. The origami band should appear as a distinct band with a slight shift as compared with the scaffold. Excess staples will have created a broader band that traveled further. Crush the gel piece with a pestle, transfer it to a Freeze 'N Squeeze column, and spin it for 6 min at 1,000g at 4 °C. Keep the flow-through and discard the filter.
- ? TROUBLESHOOTING**
- PAUSE POINT** The origami can be stored at 4 °C for 1 week or at -20 °C in LoBind tubes for long-term storage.
- Preparation of DNA origami for DNA-PAINT imaging ● TIMING ~45 min**
- 18| There are two options for preparing microscopy slides. See option A for the preparation in a custom-built flow chamber that will be sealed after immobilization of structures and addition of imager solution. For Exchange-PAINT experiments that require fluid exchange, see option B for preparation in an open chamber. The process of making custom-built chambers is also depicted in **Supplementary Figure 10**.
- (A) Immobilization in a custom-built chamber**
- Clean the microscopy slide and the cover glass with isopropanol and dry it with lab wipes.
 - Prepare a flow chamber by taping two stripes of double-sided adhesive tape ~8 mm apart on the microscopy slide and form a flow chamber by placing a cover glass on top. The resulting channel will have a volume of ~20–30 μl. Use a pipette tip and press the cover glass firmly against the sticky tape. The sticky tape will appear darker when the cover glass is in good contact.
▲ CRITICAL STEP Do not use excessive force, as the glass may break.
 - Remove excess adhesive tape by pulling the tape over the edges of the cover glass.
 - Fill the chamber with 20 μl of BSA-Biotin solution (1 mg/ml) and incubate it for 2 min.
 - Wash the channel with 40 μl of Buffer A+ by holding the tip of a folded lab wipe on one end of the channel and simultaneously pipetting in washing buffer on the other side. The capillary forces of the tissue will suck the liquid out of the chamber, whereas the pipetting will introduce additional volume. Control the flow by variation of pipetting speed and tissue pressure.
▲ CRITICAL STEP Avoid bubbles by keeping an even flow. Do not let the chamber dry out. Practice with an empty slide and water if necessary.
 - Add 20 μl of streptavidin solution (0.5 mg/ml) to the channel and incubate it for 2 min.
 - Wash the channel with 40 μl of Buffer A+.
 - Wash the channel with 40 μl of Buffer B+.
 - Add 20 μl of (5 μl of gel-purified DNA origami and 15 μl of Buffer B+) origami solution and incubate for 2 min.
? TROUBLESHOOTING
 - Wash the channel with 40 μl of Buffer B+.
 - Add 20 μl of imager solution to the channel.
▲ CRITICAL STEP Imager concentration has a critical role in proper acquisition of DNA-PAINT data. For *in vitro* samples, consider an ~5 nM imager concentration for a DNA nanostructure with 12 binding sites as a start value.
 - (Optional) For spectral multiplexing, use 2 different DNA sequences with spectrally distinct fluorophores, such as Cy3B and Atto655.
 - Use epoxy glue to seal the chamber. Pour the glue on a piece of weighing paper, mix with a pipette tip and distribute the glue evenly on the edges of the cover glass. Once the chamber is sealed, place the pipette tip standing up in the remaining epoxy to later evaluate the glue dryness.

- (xiv) Wait for ~15 min for the epoxy to dry. The drying process can be evaluated by checking the pipette tip in the epoxy. Once the epoxy is completely dry, the pipette tip should stick. The sample is now ready for imaging.

▲ **CRITICAL STEP** Wait until the epoxy is completely dry to avoid glue contamination of the microscope objective.

(B) Immobilization in a 6-channel ibidi sticky-Slide

- (i) Clean the cover glass (24 × 60 mm) with isopropanol and dry it with lab wipe.
- (ii) Attach the cover glass upside down to the sticky-Slide and press it with the help of a pipette tip against the cover glass.
- (iii) Add 80 μl of BSA–biotin solution to the channel. Tilt the slide slightly to ensure that the chamber is completely filled and incubate it for 5 min.
- (iv) Wash the channel with 180 μl of Buffer A+ by pipetting the solution into one opening and pipetting out 180 μl from the opposing opening.
- (v) Incubate 40 μl of streptavidin solution twice for 5 min.
- (vi) Wash the channel with 180 μl of Buffer A+.
- (vii) Wash the channel with 180 μl of Buffer B+.
- (viii) Incubate the DNA origami solution (20 μl of gel-purified DNA origami + 60 μl of Buffer B+) for 20 min.

? TROUBLESHOOTING

- (ix) Wash the channel two times with 100 μl of Buffer B+.
- (x) Add Imager strand solution to the sample for imaging.
▲ **CRITICAL STEP** Imager concentration has a critical role in proper acquisition of DNA-PAINT data. For *in vitro* samples, consider ~5 nM for DNA nanostructures with 12 binding sites as a start value. (Optional) For spectral multiplexing, use two different DNA sequences with spectrally distinct fluorophores, such as Cy3B and Atto655.
- (xi) Put the lid back on the chamber. The sample is now ready for imaging.

Sample preparation for *in situ* samples

19| Generate DNA-conjugated secondary antibodies. Here, two methods are presented: option A describes the use of a maleimide-PEG2-succinimidyl ester cross-linker, which links free amino groups on the protein to reduced thiolated DNA²², and option B describes the use of a DBCO-sulfo-NHS ester, which binds to amino groups on the protein and via copper-free click chemistry to an azide-modified DNA strand⁵⁵. The copper-free click chemistry allows for conjugation of multiple antibody species in parallel, whereas the attachment via Maleimide chemistry is more cost-effective, considering the DNA components. The reduction of the thiol group and the subsequent purification of the DNA from DTT using the Nap-5 column is time-consuming and time-critical. Long waiting times will lead to disulfide bridging of the DNA strands. The copper-free click chemistry in comparison does not have such a time-consuming and time-critical step in regard to the reagent stability, and therefore allows for parallel labeling of the antibodies. Alternatively, DNA-labeled antibodies can also be obtained from Ultivue (<http://www.ultivue.com>).

(A) DNA labeling of antibodies via maleimide-PEG2-succinimidyl ester for cellular labeling ● TIMING 1 d 1 h

- (i) To reduce the thiolated DNA for the Maleimide reaction, mix 30 μl of 1-mM thiolated DNA with 70 μl of freshly prepared DTT solution and incubate the mixture on a shaker for 2 h at RT covered with aluminum foil.
- (ii) Concentrate the antibody using Amicon spin filters (100 kDa). Wash the filters with 1× PBS for 10 min at 14,000g at 4 °C. Discard the flow-through, add 300 μl of antibody solution and spin at 14,000g for 5 min at 4 °C. Discard the flow-through and invert the spin filter in an empty tube. Spin for 6 min at 1,000g at 4 °C. Adjust the volume to 100 μl with 1× PBS, and measure the concentration with the NanoDrop spectrophotometer. Keep the antibody on ice. The final concentration should be >1.5 mg/ml.
- (iii) Prepare the cross-linker solution in 1× PBS and add it to the antibody in a 10:1 molar ratio. Incubate the solution for 90 min at 4 °C on a shaker covered in aluminum foil. Start the reaction 1 h after the DNA reduction step was started.
▲ **CRITICAL STEP** The desired amount of cross-linker must be no more than 5 μl in volume in order to avoid adding too much of DMF or diluting the antibody further.
- (iv) 20 min before the DNA reduction step is completed, start to equilibrate a Nap-5 column with ddH₂O filled to the top three times. Add DNA–DTT solution to the column and immediately add 400 μl of ddH₂O. After 400 μl has passed through, add 1 ml of ddH₂O and start collecting fractions immediately. Collect three drops in the first four tubes, two drops in the following four and one drop in the last eight tubes. Starting from the last collected tube, add 25 μl of BCA mix to the tubes. If DTT is still present, the solution turns purple. Discard those tubes. If no color change is visible anymore, discard the next tube as well and measure the concentration of the remaining fractions via the NanoDrop spectrophotometer. Pool the fractions with the highest concentrations. The highest fractions will have a DNA concentration between 200 and 800 ng/μl.

▲ **CRITICAL STEP** If DTT is still present in the DNA solution, it will interfere with the Maleimide reaction.

PROTOCOL

- (v) Concentrate the reduced DNA using Amicon spin filters (3 kDa). Wash the filter with 1× PBS for 30 min at 14,000g at 4 °C. Discard the flow-through and add the pooled fractions of reduced DNA to the filter. Centrifuge for 30 min at 14,000g at 4 °C and discard the flow-through. Invert the spin filter in an empty new tube and spin for 6 min at 1,000g at 4 °C. Measure the concentration with the NanoDrop spectrophotometer; the DNA should have a concentration >700 ng/μl.
- (vi) After the antibody–cross-linker reaction has completed, use a Zeba desalting column to remove the linker. Remove the storage solution by centrifugation at 1,500g for 1 min at 4 °C. Mark the side where the resin slid up, and perform the subsequent centrifugation steps in the same orientation. Wash the Zeba column with 300 μl of PBS and centrifuge it at 1,500g for 1 min at 4 °C. Dry the bottom of the column and use a fresh 1.5-ml tube. Add the antibody–cross-linker solution to the Zeba column, and spin at 1,500g for 2 min at 4 °C. Discard the Zeba column, retain the flow-through and measure the concentration with the NanoDrop spectrophotometer. The antibody concentration should be > 1.5 mg/ml.
- (vii) Incubate a 10:1 molar ratio of thiolated DNA to antibody overnight on a shaker covered in aluminum foil in a cold room.
- (viii) Remove excess DNA by Amicon spin filtration (100 kDa). For this, wash the filters with 1× PBS for 10 min at 14,000g at 4 °C. Discard the flow-through, add antibody–DNA solution, add 300 μl PBS and spin at 14,000g for 5 min at 4 °C. Discard the flow-through and invert the spin filter into an empty tube. Spin the solution for 6 min at 1,000g at 4 °C. Adjust the volume to 100 μl with 1× PBS, and measure the concentration with the NanoDrop spectrophotometer. The peak signal should be shifted toward 260 nm from 280 nm, and the concentration should be >5 mg/ml because of the stronger absorbance of DNA. Keep the antibody on ice and store it at 4 °C for a maximum of 6 months.

? TROUBLESHOOTING

(B) Labeling via DBCO-sulfo-NHS ester ● TIMING 4 h

- (i) Concentrate the antibody using Amicon spin filters (100 kDa). For this, wash the filters with 1× PBS for 10 min at 14,000g at 4 °C. Discard the flow-through, add 300 μl of antibody solution and spin at 14,000g for 5 min at 4 °C. Discard the flow-through and invert the spin filter in an empty tube. Spin for 6 min at 1,000g at 4 °C. Adjust the volume to 100 μl with 1× PBS, and measure the concentration with the NanoDrop spectrophotometer. Keep the antibody on ice. The final concentration should be >1.5 mg/ml.
- (ii) Prepare 5 μl of cross-linker solution in 1× PBS so that the final solution after addition of 100 μl of the antibody contains a 10:1 molar ratio of cross-linker to antibody. Incubate the solution for 90 min at 4 °C on a shaker covered in aluminum foil.
- (iii) After the antibody–cross-linker reaction is completed, use a Zeba desalting column to remove the linker. Remove the storage solution by centrifugation at 1,500g for 1 min at 4 °C. Mark the side where the resin slid up, and perform the subsequent centrifugation steps in the same orientation. Wash the Zeba column with 300 μl of 1× PBS at 1,500g for 1 min at 4 °C. Dry the bottom of the column and use a fresh 1.5-ml tube. Add antibody–cross-linker solution to the Zeba column and spin it at 1,500g for 2 min at 4 °C. Discard the Zeba column, retain the flow-through and measure the concentration on the NanoDrop spectrophotometer. The antibody concentration should be >1.5 mg/ml.
- (iv) Create a 15:1 molar ratio of DNA to antibody and incubate the solution for 1 h at RT on a shaker covered in aluminum foil.
- (v) Remove the excess DNA by Amicon spin filtration (100 kDa). For this, wash the filters with 1× PBS for 10 min at 14,000g at 4 °C. Discard the flow-through, add antibody–DNA solution, add 300 μl of 1× PBS and spin at 14,000g for 5 min at 4 °C. Discard the flow-through and invert the spin filter in an empty tube. Spin for 6 min at 1,000g at 4 °C. Adjust the volume to 100 μl with 1× PBS, and measure the concentration with the NanoDrop spectrophotometer. The peak signal should be shifted toward 260 nm from 280 nm, and the concentration should be >5 mg/ml because of the stronger absorbance of DNA.

? TROUBLESHOOTING

■ PAUSE POINT Keep the antibody on ice and store it at 4 °C for a maximum of 6 months.

Immunofixation of cells ● TIMING 2.5 d

▲ CRITICAL In Steps 20–33, we describe procedures for immunofixation optimized for DNA-PAINT super-resolution microscopy. Fixation strategies depend on the target of interest, as well as on the antibody-recognition motifs⁵⁷.

20| Seed 30,000 cells in 8-well chambered cover glasses, and let them grow overnight at 37 °C and 5% CO₂ in an incubator.

21| After 24 h, the cells are ready to be fixed.

22| In this step, fixative is added to the cells; this can be performed in two ways: option A, an optimized protocol for maximum preservation of cellular cytoskeletal structures (recommended for imaging microtubules) and option B, a standard protocol.

(A) Optimized microtubule fixation

- (i) Pre-extract the cells with prewarmed (37 °C for 10 min) pre-extraction buffer for 90 s.
- (ii) Remove the extraction buffer and fix the cells for 15 min in prewarmed enhanced microtubule fixative.

(B) Standard fixation

- (i) Fix the cells in standard fixative for 15 min.

23| Aspirate the fixative solution and reduce the sample with 1 mg/ml sodium borohydride for 7 min.

▲ **CRITICAL STEP** Sodium borohydride must be prepared just before application to the sample and is very volatile.

24| Wash the chamber four times (1 × 20 s, 3 × 5 min) with 1× PBS at pH 7.2.

25| Block and permeabilize the cell sample in blocking buffer for 90 min at RT.

26| Dilute the primary antibody according to supplier instructions in antibody dilution buffer, and incubate the sample at 4 °C overnight on a rocking platform.

27| Wash the sample three times for 5 min in 1× PBS.

28| Dilute DNA-labeled secondary antibody (5–50 µg/ml) in antibody dilution buffer, and apply it to the sample for 60 min. (Optional) For multiplexing experiments, use different secondary antibodies with orthogonal DNA handles; see **Supplementary Table 2** for recommended sequences.

29| Wash the sample three times for 5 min in 1× PBS.

30| Dilute 90-nm gold particles at a 1:10 ratio in PBS as fiducial markers and incubate for 5 min on the cell sample.

31| Wash the sample three times for 5 min in 1× PBS.

32| Add a target-specific imager solution to the sample.

▲ **CRITICAL STEP** Imager concentration has a critical role in proper acquisition of DNA-PAINT data. The concentration should be adjusted for the target (hence docking strand) density. For microtubules, we recommend starting with a 500 pM imager strand concentration and adjusting as necessary.

33| (Optional) For multiplexed Exchange-PAINT experiments, place the exchange lid with the connected tubing on the chambered cover glass.

Data acquisition ● TIMING 10 min to 10 hours

▲ **CRITICAL** The following section describes the procedure for performing DNA-PAINT experiments using imager sequences labeled with Cy3B fluorophores. As the SNR for DNA-PAINT is rather high, both CCD or sCMOS cameras are suitable for imaging. The procedure is written for use of an iXon Ultra DU-897 EMCCD camera, although electron-multiplying is not necessary. Considerations in regard to acquisition of images with ultra-high resolution are described in **Box 2**. For test purposes, raw DNA-PAINT data can also be simulated *in silico* with ‘Picasso: Simulate’ (see **Box 3** for procedure details).

34| Place the sample on the microscope stage, and move the objective up until the immersion oil touches the sample.

35| (Optional) For multiplexing with Exchange-PAINT, attach tubing with syringes to the exchange chamber. Consider using an ~15-ml syringe volume of exchange buffer per exchange round for *in situ* exchange experiments, and ~1 ml of exchange buffer per exchange round for *in vitro* experiments. For *in situ* experiments, additionally attach tubing to the chamber inlet. Put the connected syringes into plastic trays to avoid accidental fluid spills. The syringes should be at the same level as the chamber to avoid liquid exchange, as they are communicating vessels.

▲ **CRITICAL STEP** Handle liquids extremely carefully if they are close to the microscope. Improper handling and leakage can lead to damage of delicate microscope components.

36| Start µManager, select the configuration file for the camera and select ‘Ok’. The main window of µManager will open.

37| Set ‘Exposure [ms]’ with regard to the following considerations: exposure times for DNA-PAINT experiments are dependent on the imager length and concentration, the imaging buffer and the docking strand density of the target structure. Typical

PROTOCOL

exposure times for 9-bp DNA duplexes are hundreds of milliseconds, and those for 8-bp DNA duplexes are tens of milliseconds, as they have a shorter ON-time. For the samples used in **Figure 1**, an exposure time of 300 ms for *in vitro* (Buffer B+) and 200 ms for *in situ* (Buffer C) samples was used. ‘Picasso: Simulate’ can be used to determine ideal exposure times for given sample parameters. As a general rule of thumb, camera integration times should be matched to mean ON-times of DNA-PAINT imager/docking duplexes for best performance; these can be experimentally determined using Picasso (see Step 69B). Refer to **Supplementary Table 6** for the acquisition settings used for the images in this protocol.

38| Open ‘Tools’ > ‘Device Property Browser’.

39| Set the camera parameters: set ‘Output_Amplifier’ to ‘Conventional’, set ‘Region of Interest’ to ‘Full Image’, set ‘Frame Transfer’ to ‘On’, set ‘PixelFormat’ to ‘16bit’, set ‘ReadMode’ to ‘Image’ and set ‘Camera shutters’ to ‘Open’.

40| Click on ‘Live’ in the main window, and the ‘Snap/Live’ window will appear. Select ‘Autostretch’ in the contrast settings. The ‘Snap/Live’ window should show background noise.

41| Set the laser to a low power density of 0.25 kW/cm² at the sample plane (refer to the calibration as performed in the Equipment Setup), and open the laser shutter.

? TROUBLESHOOTING

42| Focus the image.

▲ CRITICAL STEP A focused image should show blinking diffraction-limited spots, each representing the binding and unbinding of an imager strand to its target. Adjust the contrast by dragging the black and white triangles in the ‘Contrast’ window if needed. For prefocusing, preferably use a focus-lock system such as the Nikon Perfect Focus System or, in case of *in situ* samples, prefocus with the bright-field image.

? TROUBLESHOOTING

43| Increase the laser power to a power density of ~ 2.5 kW/cm² at the sample plane.

44| Adjust the laser incident angle. When starting in an epifluorescence configuration, increase the angle until total internal reflection occurs. Continue until no more light is reflected and the signal decreases. Then, go back by decreasing the angle and optimize the SNR. When imaging structures beyond the TIRF illumination range, decrease the incident angle—potentially moving to oblique (HILO) illumination³¹—just until the structure of interest is properly illuminated. Keeping the incident angle as high as possible limits out-of-focus excitation above the target structure, which is particularly critical for DNA-PAINT, as free imager strands in solution increase background and therefore affect imaging quality adversely.

45| In the device manager, adjust the ‘Readout Mode’ to the frequency with the lowest readout noise possible for the currently selected integration time. This is usually the lowest frequency at which the readout time does not exceed the exposure time. The readout time will be displayed in ‘ReadoutTime’ and should be shorter than the ‘Exposure’ time. Please double-check that the field ‘ActualInterval-ms’, which denotes the true duration between two frames, does not exceed the exposure time.

46| Click on ‘Multi-D-Acq.’ in the main window to open the ‘Multi-Dimensional Acquisition’ window. Activate ‘Time points’ and set the ‘Number’ to the number of frames to be acquired—e.g., 7,500 for *in vitro* samples and 15,000 for *in situ* samples. These exemplar numbers for total acquisition frames are suggestions for initial experiments and may have to be adjusted according to the specific experiment. For a detailed discussion of optimal acquisition time, refer to Nieuwenhuizen *et al.*¹⁶ and respective sections in the introduction of this protocol.

47| Set the interval to ‘0’ and ‘ms’. Set ‘Acquisition Order’ to ‘Time’. Activate ‘Save images’ and set a destination filename and folder.

48| Select ‘Acquire!’ to start the acquisition. A live image will pop up. The progress of the acquisition can be followed on the upper left corner.

? TROUBLESHOOTING

49| (Optional) Multiplexed image acquisition. There are two methods for performing multiplexed target acquisition with DNA-PAINT. Spectral multiplexing (option A) uses spectrally distinct fluorophores, whereas Exchange-PAINT multiplexing

(option B) uses (typically) the same fluorophore attached to orthogonal DNA species that are sequentially supplied to the sample. With Exchange-PAINT, only one species is present in the imager buffer in each multiplexing round, and it will be washed out afterward. Option A provides a relatively fast workflow for imaging multiple targets by imaging in multiple emission channels. Option B has almost no limitation in multiplexing but requires a fluid exchange system. In addition, option B provides the capability of using the most favorable fluorophore for all targets. Refer to **Supplementary Table 7** for a list of dye recommendations for DNA-PAINT.

(A) Spectral multiplexing

- (i) Perform Steps 34–48 for the first fluorophore.
 - ▲ **CRITICAL STEP** To reduce photodamage, start acquisition with the dye that has the longest excitation wavelength, and then proceed to those with shorter wavelengths.
- (ii) After acquisition of the first imager species, change the laser line and the filter set on the microscope to match the next wavelength.
- (iii) Click on 'Live' in the main window of μ Manager and adjust the TIRF angle if necessary.
- (iv) Adjust the file name in the 'Multi-Dimensional Acquisition' window.
- (v) Select 'Acquire!' to start a new acquisition.
- (iv) (Optional) Repeat the procedure for any other spectrally distinct imager species in solution.

(B) Exchange multiplexing

- (i) Perform Steps 34–48 to acquire a movie for the first imager species.
- (ii) Click on 'Live' in the main window and adjust the contrast so that individual blinking events are visible. Deselect 'Autostretch'. It is important to keep the contrast to determine when all imagers are washed out.
- (iii) Apply several washing steps while observing the 'Live/Snap' window until no more blinking events are visible. One washing step consists of filling the chamber by adding exchange buffer (for *in vitro* imaging use $\sim 180 \mu\text{l}$, and for *in situ* imaging use 1 ml) to the inlet and then removing the same volume from the outlet. For *in situ* imaging a total of ~ 15 ml and for *in vitro* imaging a total of ~ 1 ml of exchange buffer will be needed per exchange round.
 - ▲ **CRITICAL STEP** Do not remove all liquid from the chamber; it should never dry out. Perform liquid exchange slowly to avoid introducing air bubbles into the chamber or disturbing the sample.
- ? **TROUBLESHOOTING**
- (iv) After washing, introduce a new imager solution into the chamber. For *in vitro* samples, simply pipette the required amount into the chamber and remove the same amount from the outlet. For *in situ* samples, empty the inlet tubing by disconnecting the empty syringe and pumping air through it. Connect a new 2-ml syringe with a new imager solution and fill the chamber.
- (v) While introducing the new imager, the 'Live/Snap' window should show reappearing blinking events.
- (vi) Adjust the filename in the 'Multi-Dimensional Acquisition' window.
- (vii) Select 'Acquire!' to start a new acquisition.
- (viii) (Optional) Repeat the procedure for subsequent imaging rounds.

Image reconstruction ● **TIMING 5–30 min**

50| Identification and fitting of single-molecule spots. In 'Picasso: Localize', open a movie file by dragging the file into the window or by selecting 'File' > 'Open'. If the movie is split into multiple μ Manager .tif files, open only the first file. Picasso will automatically detect the remaining files according to their file names.

51| Adjust the image contrast (select 'View' > 'Contrast') so that the single-molecule spots are clearly visible.

52| To adjust spot identification and fit parameters, open the 'Parameters' dialog (select 'Analyze' > 'Parameters').

53| In the 'Identification' group, set the 'Box side length' to the rounded integer value of $6 \times \sigma + 1$, where σ is the standard deviation of the PSF. In an optimized microscope setup, σ is one pixel, and the respective 'Box side length' should be set to 7. The value of 'Min. net gradient' specifies a minimum threshold above which spots should be considered for fitting. The net gradient value of a spot is roughly proportional to its intensity, independent of its local background. By checking 'Preview', the spots identified with the current settings will be marked in the displayed frame. Adjust 'Min. net gradient' to a value at which only spots are detected (no background).

54| In the 'Photon conversion' group, adjust 'EM Gain', 'Baseline', 'Sensitivity' and 'Quantum Efficiency' according to your camera specifications and the experimental conditions. Set 'EM Gain' to 1 for conventional output amplification. 'Baseline' is

PROTOCOL

the average dark camera count. ‘Sensitivity’ is the conversion factor (electrons per analog-to-digital (A/D) count) and ‘Quantum Efficiency’ should be set according to the average emission wavelength.

▲ **CRITICAL STEP** These parameters are critical to converting camera counts to photons correctly. The quality of the upcoming maximum likelihood fit strongly depends on a Poisson photon noise model, and thus on the absolute photon count.

For simulated data, generated with ‘Picasso: Simulate’ as described in **Box 3** and **Figure 7**, set the parameters as follows: ‘EM Gain’ = 1, ‘Baseline’ = 0, ‘Sensitivity’ = 1, ‘Quantum Efficiency’ = 1.

55| From the menu bar, select ‘Analyze’ > ‘Localize (Identify & Fit)’ to start spot identification and fitting in all movie frames. The status of this computation is displayed in the window’s status bar. After completion, the fit results will be saved in a new file in the same folder as the movie, in which the filename is the base name of the movie file with the extension ‘_locs.hdf5’. Furthermore, information about the movie and analysis procedure will be saved in an accompanying file with the extension ‘_locs.yaml’; this file can be inspected using a text editor.

56| *Rendering of the super-resolution image:* In ‘Picasso: Render’, open a movie file by dragging a localization file (ending with ‘.hdf5’) into the window or by selecting ‘File’ > ‘Open’. The super-resolution image will be rendered automatically. A region of choice can be zoomed into by a rectangular selection using the left mouse button. The ‘View’ menu contains more options for zooming and panning.

57| (Optional) Adjust rendering options by selecting ‘View’ > ‘Display Settings’. The field ‘Oversampling’ defines the number of super-resolution pixels per camera pixel. The contrast settings ‘Min. Density’ and ‘Max. Density’ define at which number of localizations per super-resolution pixel the minimum and maximum color of the colormap should be applied.

58| (Optional) For multiplexed image acquisition, open HDF5 localization files from other channels subsequently. Alternatively, drag and drop all HDF5 files to be displayed simultaneously.

Image post-processing: drift correction ● **TIMING** seconds to minutes

59| Picasso offers two procedures to correct for drift: an RCC algorithm⁶⁶ (option A), and use of specific structures in the image as drift markers²³ (option B). Although option A does not require any additional sample preparation, option B depends on the presence of either fiducial markers or inherently clustered structures in the image. On the other hand, option B often supports more precise drift estimation and thus allows for higher image resolution. To achieve the highest possible resolution (ultra-resolution), we recommend consecutive applications of option A and multiple rounds of option B. The drift markers for option B can be features of the image itself (e.g., protein complexes or DNA origami) or intentionally included markers (e.g., DNA origami or gold nanoparticles). When using DNA origami as drift markers, the correction is typically applied in two rounds: first, with whole DNA origami structures as markers, and, second, using single DNA-PAINT binding sites as markers. In both cases, the precision of drift correction strongly depends on the number of selected drift markers.

(A) Redundant cross-correlation drift correction

- (i) In ‘Picasso: Render’, select ‘Postprocess’ > ‘Undrift by RCC’.
- (ii) A dialog will appear asking for the segmentation parameter. Although the default value, 1,000 frames, is a sensible choice for most movies, it might be necessary to adjust the segmentation parameter of the algorithm, depending on the total number of frames in the movie and the number of localizations per frame⁶⁶. A smaller segment size results in better temporal drift resolution but requires a movie with more localizations per frame.
- (iii) After the algorithm finishes, the estimated drift will be displayed in a pop-up window and the display will show the drift-corrected image.

(B) Marker-based drift correction

- (i) In ‘Picasso: Render’, pick drift markers as described in Steps 61–64. Use the ‘Pick similar’ option (Step 65) to automatically detect a large number of drift markers similar to a few manually selected ones.
▲ **CRITICAL STEP** If the structures used as drift markers have an intrinsic size larger than the precision of individual localizations (e.g., DNA origami, large protein complexes), it is critical to select a large number of structures. Otherwise, the statistic for calculating the drift in each frame (the mean displacement of localization to the structure’s center of mass) is not valid.
- (ii) Select ‘Postprocess; > ‘Undrift from picked’ to compute and apply the drift correction.

60| (Optional) Save the drift-corrected localizations by selecting ‘File’ > ‘Save localizations’.

Picking of regions of interest ● **TIMING 5–30 min**

- 61** | *Manual selection.* Open 'Picasso: Render' and load the localization HDF5 file to be processed.
- 62** | Switch the active tool by selecting 'Tools' > 'Pick'. The mouse cursor will now change to a circle.
- 63** | Set the size of the pick circle by adjusting the 'Diameter' field in the tool settings dialog ('Tools' > 'Tools Settings').
- 64** | Pick regions of interest using the circular mouse cursor by clicking the left mouse button. All localizations within the circle will be selected for further processing.
- 65** | *(Optional) Automated region of interest selection.* Select 'Tools' > 'Pick similar' to automatically detect and pick structures that have similar numbers of localizations and RMS deviation (RMSD) from their center of mass than already-picked structures. The upper and lower thresholds for these similarity measures are the respective standard deviations of already-picked regions, scaled by a tunable factor. This factor can be adjusted using the field 'Tools' > 'Tools Settings' > 'Pick similar ± range'. To display the mean and standard deviation of localization number and RMSD for currently picked regions, select 'View' > 'Show info' and click 'Calculate info below'.
- 66** | *(Optional) Exporting of pick information.* All localizations in picked regions can be saved by selecting 'File' > 'Save picked localizations'. The resulting HDF5 file will contain a new integer column 'group' indicating to which pick each localization is assigned.
- 67** | *(Optional) Statistics about each pick region can be saved by selecting 'File' > 'Save pick properties'.* The resulting HDF5 file is not a localization file. Instead, it holds a data set called 'groups' in which the rows show statistical values for each pick region.
- 68** | *(Optional) The picked positions and diameter itself can be saved by selecting 'File' > 'Save pick regions'.* Such saved pick information can also be loaded into 'Picasso: Render' by selecting 'File' > 'Load pick regions'.

Additional post-processing steps

69 | Depending on the experimental goals, a variety of post-processing steps may be used. To filter localizations based on their properties, for example to remove localizations below a certain photon threshold, use option A. For investigating the statistics of DNA-PAINT binding kinetics and how to count DNA-PAINT binding sites with qPAINT²², use options B and C, respectively. Option D describes the procedure to generate an average image of multiple structures. Finally, option E describes the procedure to align images from multiplexed experiments.

(A) Filtering of localizations ● **TIMING 5–10 min**

- (i) Open a localization HDF5 file in 'Picasso: Filter' by dragging it into the main window or by selecting 'File' > 'Open'. The displayed table shows the properties of each localization in rows. Each column represents one property (e.g., coordinates, number of photons); see the **Supplementary Manual** for details.
- (ii) To display a histogram from values of one property, select the respective column in the header and select 'Plot' > 'Histogram' (Ctrl + h). 2D histograms can be displayed by selecting two columns (press Ctrl to select multiple columns) and then selecting 'Plot' > '2D Histogram' (Ctrl + d).
- (iii) Left-click and hold the mouse button down to drag a selection area in a 1D or 2D histogram. The selected area will be shaded in green, as shown in **Supplementary Figure 5b,c**. Each localization event with histogram properties outside the selected area is immediately removed from the localization list.
- (iv) Save the filtered localization table by selecting 'File' > 'Save'.

(B) Analysis of blinking kinetics ● **TIMING 5–60 min**

- (i) In 'Picasso: Render', pick regions of interest as described in Steps 61–65.
- (ii) Select 'View' > 'Show info'.
- (iii) In the opened dialog, click 'Calculate info below'. The mean and standard deviation per pick of several values will be calculated and displayed. The 'Length' row describes the blinking 'ON' time (τ_b) and the 'Dark time' row describes the blinking 'OFF' time (τ_d).
- (iv) Click 'Histograms' to open a new window showing histograms for the picked region's kinetics.
- (v) *(Optional) Individual values for each picked region can be obtained by exporting the data.* Select 'File' > 'Save pick properties'. The saved HDF5 file will contain a data set called 'groups', in which each row corresponds to one pick region.

(C) Counting of molecule numbers with qPAINT ● TIMING 5–60 min

- (i) In ‘Picasso: Render’, pick calibration regions as described in Steps 61–64. Typically, calibration regions are regions with a known number of binding sites. Do not use the option ‘Pick similar’ (Step 65), as this may bias the calibration.
- (ii) Select ‘View’ > ‘Show info’ and click ‘Calculate info below’.
- (iii) Set ‘# Units per pick’ to the number of units to which the counting should be calibrated. Typically, one unit is equal to one DNA-PAINT binding site, but other user-defined units might be suitable too. This could, i.e., be useful in the case in which calibration is performed on single antibodies, which can carry multiple docking strands for protein quantification using qPAINT. The final counting result will be reported in number of units. For example, if the calibration regions contain 12 binding sites and the counting result should be reported in ‘number of binding sites’, then ‘# Units per pick’ should be set to 12.
- (iv) Click ‘Calibrate influx’ for an estimation of the influx rate from the calibration regions kinetics. The influx rate will be displayed in the respective field. As an alternative to the experimental calibration, the influx rate (ξ) can be theoretically calculated via $\xi = k_{\text{on}} \times c$ if the ON rate (k_{on}) and imager concentration (c) are known. In that case, enter the influx rate manually into the respective field.
- (v) Select ‘Tools’ > ‘Clear picks’ to remove the calibration pick selections.
- (vi) Pick structures of interest (Steps 61–65) from which the unknown number of units should be determined.
- (vii) In the ‘Info’ dialog, click ‘Calculate info below’. The mean number of units per picked region will be displayed in the ‘# Units’ row, as calculated from the currently displayed influx rate.
- (viii) (Optional) The individual number of units for each picked region can be obtained by exporting pick property data. Select ‘File’ > ‘Save pick properties’. The saved HDF5 file will contain a data set called ‘groups’, which holds statistics about each pick region as rows, including a column for the unit number (‘n_units’).

(D) Particle averaging ● TIMING 10–30 min

- (i) In ‘Picasso: Render’, pick structures to be averaged as in Steps 61–65.
- (ii) Save the picked localizations by selecting ‘File’ > ‘Save picked localizations’.
- (iii) Load the resulting file with picked localizations into ‘Picasso: Average’ by selecting ‘File’ > ‘Open’ or dragging and dropping it into the window.
- (iv) ‘Picasso: Average’ will immediately perform a translational alignment of the picked structures and display an average image. Rotational and refined translational alignment will follow in the next steps.
- (v) Select ‘Process’ > ‘Parameters’ and adjust the ‘Oversampling’ parameter. We recommend choosing the highest number at which the average image still appears smooth. High oversampling values result in substantial computational time. Hence, it might be useful to first use low oversampling to generate a less-refined average image and perform a second averaging step with higher oversampling for optimized resolution.
- (vi) Adjust the number of average iterations in the ‘Iterations’ field. In most cases, a value of 10 is more than sufficient. If you are unsure about the computational time of the process, choose one iteration as a starting point. More iterations can be added later by repeating the processing steps. After a certain number of iterations, the average image will converge, meaning that it will not change with more iterations.
- (vii) Select ‘Process’ > ‘Average’ to perform particle averaging with the current oversampling for the set number of iterations. This step can be repeated with different settings. The program will use the current average image as a starting point.
- (viii) Once the average image has converged, save the transformed localizations by selecting ‘File’ > ‘Save’. The resulting HDF5 localization file contains the aligned localizations in the center of the movie dimensions. It can be loaded like any other HDF5 localization file into ‘Picasso: Render’.

(E) Aligning of channels from multiplexed experiments ● TIMING 5–10 min

- (i) To align images from multiplexed data acquisition, the images need to share some features as reference points. Such reference features can be the cell shape for *in situ* images (typically, background is higher inside the cell) or overlapping clusters (for example, on the same DNA origami). If alignment results are ambiguous or not satisfying because of the lack of inherent reference features, drift or alignment markers should be included and imaged in all channels.
- (ii) In ‘Picasso: Render’ display all HDF5 localization files to be aligned.
- (iii) (Optional) If the reference features are too weak to create proper alignment, they can be selected manually, as described in Steps 61–65. Ensure that within a picked region the reference structures of all channels are included.
- (iv) Select ‘Postprocess’ > ‘Align’.
- (v) (Optional) Export the aligned localizations by selection ‘File’ > ‘Save localizations’.

? TROUBLESHOOTING

Troubleshooting advice can be found in **Table 1**.

TABLE 1 | Troubleshooting table.

Steps	Problem	Possible reason	Solution
Sample preparation			
Step 17	There is no band visible on the gel	Depending on the used final scaffold concentration, the bands can appear very faint on the blue-light transilluminator table and seem difficult to excise	To improve brightness of the sample band, use a more sensitive DNA stain such as SYBR Gold, or increase scaffold concentration
	The structure does not fold	Thermal gradients have an important role during the assembly process of DNA nanostructures. However, the rectangle 2D origami design shows extremely robust folding behavior and forms with high yield within ~75 min	Different temperature gradients between 15 and 72 h can be used to improve folding performance. Prepare fresh staple stocks for the origami structure with particular focus on correct magnesium concentration and staple excess
Step 18A(ix), 18B(viii)	There are not enough DNA origami structures on the surface	Depending on the purification method, different origami concentrations are obtained—e.g., the size of the excised gel band will influence the concentration after the Freeze 'N Squeeze column purification step	Compensate for this by incubating with a higher origami concentration and/or increased incubation time. Concentration adjustment can be estimated by counting the number of targets on the surface and interpolating to the desired density. A good sample density can be achieved by incubation with 125–500 pM of origami. Typical concentrations after gel purification are between 1 and 2 nM, and those after PEG purification are approximately 8–10 nM. Alternatively, the DNA origami solution can be incubated longer (up to 45 min)
Step 19A(viii), 19B(v)	After purification, there still seem to be free DNA strands in solution	The DNA strands might not be completely filtered out by the spin columns, which are optimized for protein concentration	For further purification of DNA-labeled antibodies, use size-exclusion column chromatography to remove the free DNA (with a Superdex 75/200)
	Not enough DNA strands are attached to the antibodies	Not enough cross-linker or DNA was used	For more DNA handles attached to the antibodies, use larger excess of cross-linker (40×) and DNA (30×). However, please note that an increased DNA-to-antibody ratio might lead to reduced binding affinity of antibodies or increased off-target binding
Data acquisition			
Step 41	Poor data quality	Laser power not adjusted to sample	To achieve the best possible data quality, it is important to extract the largest possible number of photons from a single binding (blinking) event of the fluorophores. A good indicator of a suitable laser power setting can be estimated by measuring the bright time versus laser power. Increase laser power until the bright time decreases. What happens is that imager strands start to bleach while they are still bound to docking strands. This should be the upper limit of your laser power setting. When a laser power meter is available, a good reference value for power densities in DNA-PAINT experiments using, i.e., Cy3B as dye and 561-nm laser excitation is 1–6 kW/cm ²
Step 42	The focal plane is difficult to find	Focusing was not performed in bright-field mode, or the immersion oil was not in contact with the cover glass.	For cellular samples, focusing should be performed in bright-field. For DNA nanostructures, the immersion oil on the objective should touch the cover glass; use oblique illumination and then slowly raise the objective until the surface of the cover glass is reached. Monitor the approach in 'Live' mode. Reaching the cover glass will be visible via an increase in fluorescence and appearance of diffraction-limited blinking spots. Add fluorescent beads that have increased brightness to find the focal plane, if necessary

(continued)

PROTOCOL

TABLE 1 | Troubleshooting table (continued).

Steps	Problem	Possible reason	Solution
Step 48	The sample drifts in xy and/or focus is lost during image acquisition	Setup not equilibrated	Before image acquisition, allow the sample to 'equilibrate' on the microscope for 5–15 min. Adjust room temperature to maintain a constant ambient temperature to avoid additional thermal drift of microscope and stage components
Step 49B(iii)	The imager strands are difficult to wash away	Cellular samples are highly cross-linked through the fixation process. Imager strands might be trapped in the cross-linked network	We recommend incubating with the washing solution for 3 min so that the imager strands can diffuse into the large reservoir. In addition, washing with gentle flow can be effective
Box 3, step 6	The simulation of a DNA-PAINT data set takes a long time	The time required to simulate data sets is dependent on the number of structures, imager concentration, frames and image size	As computation time increases with image size, it is recommended to avoid exceeding an image size of 64 × 64 pixels. A simulation with the standard settings should take <1 min on the described analysis computer

● TIMING

Steps 1–5, design of DNA nanostructures: 1 h

Steps 6–9, folding of DNA nanostructures: 6–7 h

Steps 10–17, purification of DNA nanostructures: ~3.5 h

Step 18, preparation of DNA origami for DNA-PAINT imaging: 45 min

Step 19A, preparation of DNA-labeled antibodies using maleimide-PEG2-succinimidyl ester: 1 d and 1 h

Step 19B, labeling via DBCO-sulfo-NHS ester: 4 h

Steps 20–33, immunofixation of cells: 2.5 d

Steps 34–49, data acquisition: 10 min to 10 h; for each multiplexing round ~20 min–2 h

Steps 50–58, image reconstruction: 5–30 min

Steps 59 and 60, drift correction: seconds to minutes

Steps 61–68, picking of regions of interest: 5–30 min

Step 69A, filtering of localizations: 5–10 min

Step 69B, analysis of blinking kinetics with qPAINT: 5–60 min

Step 69C, counting of molecule numbers with qPAINT: 5–60 min

Step 69D, particle averaging: 10–30 min

Step 69E, aligning of channels for multiplexed experiments: 5–10 min

Box 1, construction of a fluid exchange chamber for *in situ* imaging: 30 min

Box 2, ultra-resolution imaging: ~7 h

Box 3, *in silico* simulation of DNA-PAINT: 10–60 min

ANTICIPATED RESULTS

Examples of single-color DNA-PAINT super-resolution images can be found in **Figure 1**. Panel **b** presents an image of a DNA origami with a three-by-four grid of binding sites, as designed with 'Picasso: Design'. Measured distances between individual binding sites are in good agreement with the designed origami. Panels **d** and **e** show a DNA-PAINT image of microtubules *in situ*, immunolabeled with primary and secondary antibodies. Hollow microtubule structures, observed here as two parallel lines because of the 2D projection, are characteristic for a high labeling density and localization precision.

Expected results for multiplexed DNA-PAINT experiments by Exchange-PAINT are shown in **Figure 2**. Panels **d**, **e** and **f** show *in vitro* DNA origami imaged with multiple 'Exchange' rounds before (**d**) and after (**e**, **f**) alignment. The image after alignment shows that the DNA nanostructure is in good agreement with the designed pattern of binding sites. *In situ* Exchange-PAINT images of microtubules and Tom20, which localizes to mitochondria, are shown in panel **g**. The inset in panel **g** shows gold particles imaged in both rounds and demonstrates the alignment steps for the two images. The gold particles colocalize after the alignment procedure, and the different channels do not comprise any cross talk between them.

Results for counting DNA-PAINT binding sites via quantitative PAINT (qPAINT) can be found in **Figure 3**. Visual inspection of individual origami structures shows they match the predicted binding sites from the qPAINT analysis.

Expected results for ultra-resolution imaging, including the intermediate steps for drift correction and a final image from averaging multiple structures, can be seen in **Figure 4**. Key features of a successful ultra-resolution experiment are very high NeNA localization precision (~1 to 1.5 nm) and the ability to visually separate individual binding sites spaced 5 nm apart on the origami structures.

Note: Any Supplementary Information and Source Data files are available in the online version of the paper.

ACKNOWLEDGMENTS We thank B. Rieger, S.S. Agasti, S. Strauss, D. Haas, J.B. Woehrstein and E. Woehrstein for helpful discussions. This work was supported by the German Research Foundation (DFG) through an Emmy Noether Fellowship (DFG JU 2957/1-1), the European Research Council (ERC) through an ERC Starting Grant (MolMap, grant agreement no. 680241), the Max Planck Society, the Max Planck Foundation and the Center for Nanoscience (CeNS). M.T.S. acknowledges support from the International Max Planck Research School for Molecular and Cellular Life Sciences (IMPRS-LS). T.S. acknowledges support from the DFG through the Graduate School of Quantitative Biosciences Munich (QBM). F.S. acknowledges support from the DFG through the SFB 1032 (Nanoagents for the spatiotemporal control of molecular and cellular reactions).

AUTHOR CONTRIBUTIONS J.S. and M.T.S. contributed equally to this work. J.S. designed and developed the Picasso software suite. M.T.S. developed ‘Picasso: Design’ and ‘Simulate’ and performed *in vitro* experiments. T.S. developed antibody labeling strategies and performed *in situ* experiments. F.S. performed ultra-resolution experiments. R.J. conceived the study and supervised the project. All authors contributed to the writing of the manuscript.

COMPETING FINANCIAL INTERESTS The authors declare competing financial interests: details are available in the [online version of the paper](#).

Reprints and permissions information is available online at <http://www.nature.com/reprints/index.html>. Publisher’s note: Springer Nature remains neutral with regard to jurisdictional claims in published maps and institutional affiliations.

1. Gustafsson, M.G.L. Nonlinear structured-illumination microscopy: wide-field fluorescence imaging with theoretically unlimited resolution. *Proc. Natl. Acad. Sci. USA* **102**, 13081–13086 (2005).
2. Hell, S.W. & Wichmann, J. Breaking the diffraction resolution limit by stimulated emission: stimulated-emission-depletion fluorescence microscopy. *Opt. Lett.* **19**, 780–782 (1994).
3. Betzig, E. *et al.* Imaging intracellular fluorescent proteins at nanometer resolution. *Science* **313**, 1642–1645 (2006).
4. Hess, S.T., Girirajan, T.P.K. & Mason, M.D. Ultra-high resolution imaging by fluorescence photoactivation localization microscopy. *Biophys. J.* **91**, 4258–4272 (2006).
5. Rust, M.J., Bates, M. & Zhuang, X. Sub-diffraction-limit imaging by stochastic optical reconstruction microscopy (STORM). *Nat. Methods* **3**, 793–795 (2006).
6. Heilemann, M. *et al.* Subdiffraction-resolution fluorescence imaging with conventional fluorescent probes. *Angew. Chem. Int. Ed. Engl.* **47**, 6172–6176 (2008).
7. Hell, S.W. Far-field optical nanoscopy. *Science* **316**, 1153–1158 (2007).
8. Sengupta, P. *et al.* Probing protein heterogeneity in the plasma membrane using PALM and pair correlation analysis. *Nat. Methods* **8**, 969–975 (2011).
9. Xu, K., Zhong, G. & Zhuang, X. Actin, spectrin, and associated proteins form a periodic cytoskeletal structure in axons. *Science* **339**, 452–456 (2012).
10. Honigsmann, A. *et al.* Phosphatidylinositol 4,5-bisphosphate clusters act as molecular beacons for vesicle recruitment. *Nat. Struct. Mol. Biol.* **20**, 679–686 (2013).
11. Li, D. *et al.* ADVANCED IMAGING. Extended-resolution structured illumination imaging of endocytic and cytoskeletal dynamics. *Science* **349**, aab3500 (2015).
12. Galiani, S. *et al.* Super-resolution microscopy reveals compartmentalization of peroxisomal membrane proteins. *J. Biol. Chem.* **291**, 16948–16962 (2016).
13. Hell, S.W. *et al.* The 2015 super-resolution microscopy roadmap. *J. Phys. D Appl. Phys.* **48**, 443001 (2015).
14. Huang, B., Bates, M. & Zhuang, X. Super-resolution fluorescence microscopy. *Annu. Rev. Biochem.* **78**, 993–1016 (2009).
15. Lippincott-Schwartz, J., Jennifer, L.-S. & Patterson, G.H. Photoactivatable fluorescent proteins for diffraction-limited and super-resolution imaging. *Trends Cell Biol.* **19**, 555–565 (2009).
16. Nieuwenhuizen, R.P.J. *et al.* Measuring image resolution in optical nanoscopy. *Nat. Methods* **10**, 557–562 (2013).
17. Sharonov, A. & Hochstrasser, R.M. Wide-field subdiffraction imaging by accumulated binding of diffusing probes. *Proc. Natl. Acad. Sci. USA* **103**, 18911–18916 (2006).

18. Giannone, G. *et al.* Dynamic superresolution imaging of endogenous proteins on living cells at ultra-high density. *Biophys. J.* **99**, 1303–1310 (2010).
19. Jungmann, R. *et al.* Single-molecule kinetics and super-resolution microscopy by fluorescence imaging of transient binding on DNA origami. *Nano Lett.* **10**, 4756–4761 (2010).
20. Jungmann, R. *et al.* Multiplexed 3D cellular super-resolution imaging with DNA-PAINT and Exchange-PAINT. *Nat. Methods* **11**, 313–318 (2014).
21. Iinuma, R. *et al.* Polyhedra self-assembled from DNA tripods and characterized with 3D DNA-PAINT. *Science* **344**, 65–69 (2014).
22. Jungmann, R. *et al.* Quantitative super-resolution imaging with qPAINT. *Nat. Methods* **13**, 439–442 (2016).
23. Dai, M., Jungmann, R. & Yin, P. Optical imaging of individual biomolecules in densely packed clusters. *Nat. Nanotechnol.* **11**, 798–807 (2016).
24. Schlichthaerle, T., Strauss, M.T., Schueder, F., Woehrstein, J.B. & Jungmann, R. DNA nanotechnology and fluorescence applications. *Curr. Opin. Biotechnol.* **39**, 41–47 (2016).
25. Agasti, S. *et al.* DNA-barcoded labeling probes for highly multiplexed Exchange-PAINT imaging. *Chem. Sci.* (2017) <http://dx.doi.org/10.1039/c6sc05420j>.
26. Rasnik, I., McKinney, S.A. & Ha, T. Nonblinking and long-lasting single-molecule fluorescence imaging. *Nat. Methods* **3**, 891–893 (2006).
27. Aitken, C.E., Marshall, R.A. & Puglisi, J.D. An oxygen scavenging system for improvement of dye stability in single-molecule fluorescence experiments. *Biophys. J.* **94**, 1826–1835 (2008).
28. Ha, T. & Tinnefeld, P. Photophysics of fluorescent probes for single-molecule biophysics and super-resolution imaging. *Annu. Rev. Phys. Chem.* **63**, 595–617 (2012).
29. Ries, J., Kaplan, C., Platonova, E., Eghlidi, H. & Ewers, H. A simple, versatile method for GFP-based super-resolution microscopy via nanobodies. *Nat. Methods* **9**, 582–584 (2012).
30. Opazo, F. *et al.* Aptamers as potential tools for super-resolution microscopy. *Nat. Methods* **9**, 938–939 (2012).
31. Tokunaga, M., Imamoto, N. & Sakata-Sogawa, K. Highly inclined thin illumination enables clear single-molecule imaging in cells. *Nat. Methods* **5**, 159–161 (2008).
32. Legant, W.R. *et al.* High-density three-dimensional localization microscopy across large volumes. *Nat. Methods* **13**, 359–365 (2016).
33. Rothmund, P.W.K. Folding DNA to create nanoscale shapes and patterns. *Nature* **440**, 297–302 (2006).
34. Seeman, N.C. Nucleic acid junctions and lattices. *J. Theor. Biol.* **99**, 237–247 (1982).
35. Seeman, N.C. An overview of structural DNA nanotechnology. *Mol. Biotechnol.* **37**, 246–257 (2007).
36. Douglas, S.M. *et al.* Rapid prototyping of 3D DNA-origami shapes with caDNAno. *Nucleic Acids Res.* **37**, 5001–5006 (2009).
37. Benson, E. *et al.* DNA rendering of polyhedral meshes at the nanoscale. *Nature* **523**, 441–444 (2015).
38. Kim, D.-N., Kilchherr, F., Dietz, H. & Bathe, M. Quantitative prediction of 3D solution shape and flexibility of nucleic acid nanostructures. *Nucleic Acids Res.* **40**, 2862–2868 (2012).
39. Douglas, S.M. *et al.* Self-assembly of DNA into nanoscale three-dimensional shapes. *Nature* **459**, 414–418 (2009).
40. Martin, T.G. & Dietz, H. Magnesium-free self-assembly of multi-layer DNA objects. *Nat. Commun.* **3**, 1103 (2012).
41. Sobczak, J.-P.J., Martin, T.G., Gerling, T. & Dietz, H. Rapid folding of DNA into nanoscale shapes at constant temperature. *Science* **338**, 1458–1461 (2012).
42. Bellot, G., Gaëtan, B., McClintock, M.A., Chenxiang, L. & Shih, W.M. Recovery of intact DNA nanostructures after agarose gel-based separation. *Nat. Methods* **8**, 192–194 (2011).
43. Lin, C., Perrault, S.D., Kwak, M., Graf, F. & Shih, W.M. Purification of DNA-origami nanostructures by rate-zonal centrifugation. *Nucleic Acids Res.* **41**, e40 (2013).
44. Stahl, E., Martin, T.G., Praetorius, F. & Dietz, H. Facile and scalable preparation of pure and dense DNA origami solutions. *Angew. Chem. Int. Ed. Engl.* **53**, 12735–12740 (2014).
45. Steinhauer, C., Jungmann, R., Sobey, T.L., Simmel, F.C. & Tinnefeld, P. DNA origami as a nanoscopic ruler for super-resolution microscopy. *Angew. Chem. Int. Ed. Engl.* **48**, 8870–8873 (2009).
46. Schmied, J.J. *et al.* DNA origami-based standards for quantitative fluorescence microscopy. *Nat. Protoc.* **9**, 1367–1391 (2014).
47. Dean, K.M. & Palmer, A.E. Advances in fluorescence labeling strategies for dynamic cellular imaging. *Nat. Chem. Biol.* **10**, 512–523 (2014).

48. Dempsey, G.T., Vaughan, J.C., Chen, K.H., Bates, M. & Zhuang, X. Evaluation of fluorophores for optimal performance in localization-based super-resolution imaging. *Nat. Methods* **8**, 1027–1036 (2011).
49. Mikhaylova, M. *et al.* Resolving bundled microtubules using anti-tubulin nanobodies. *Nat. Commun.* **6**, 7933 (2015).
50. Los, G.V. *et al.* HaloTag: a novel protein labeling technology for cell imaging and protein analysis. *ACS Chem. Biol.* **3**, 373–382 (2008).
51. Keppler, A., Pick, H., Arrivoli, C., Vogel, H. & Johnsson, K. Labeling of fusion proteins with synthetic fluorophores in live cells. *Proc. Natl. Acad. Sci. USA* **101**, 9955–9959 (2004).
52. Wang, L., Xie, J. & Schultz, P.G. Expanding the genetic code. *Annu. Rev. Biophys. Biomol. Struct.* **35**, 225–249 (2006).
53. Schweller, R.M. *et al.* Multiplexed *in situ* immunofluorescence using dynamic DNA complexes. *Angew. Chem. Int. Ed. Engl.* **51**, 9292–9296 (2012).
54. Ullal, A.V. *et al.* Cancer cell profiling by barcoding allows multiplexed protein analysis in fine-needle aspirates. *Sci. Transl. Med.* **6**, 219ra9 (2014).
55. Gong, H. *et al.* Simple method to prepare oligonucleotide-conjugated antibodies and its application in multiplex protein detection in single cells. *Bioconjug. Chem.* **27**, 217–225 (2016).
56. Xu, K., Babcock, H.P. & Zhuang, X. Dual-objective STORM reveals three-dimensional filament organization in the actin cytoskeleton. *Nat. Methods* **9**, 185–188 (2012).
57. Whelan, D.R. & Bell, T.D.M. Image artifacts in single molecule localization microscopy: why optimization of sample preparation protocols matters. *Sci. Rep.* **5**, 7924 (2015).
58. Edelstein, A.D. *et al.* *J. Biol. Methods* **1**, 10 (2014).
59. Beier, H.T. & Ibey, B.L. Experimental comparison of the high-speed imaging performance of an EM-CCD and sCMOS camera in a dynamic live-cell imaging test case. *PLoS One* **9**, e84614 (2014).
60. Huang, F. *et al.* Video-rate nanoscopy using sCMOS camera-specific single-molecule localization algorithms. *Nat. Methods* **10**, 653–658 (2013).
61. Shroff, H., Galbraith, C.G., Galbraith, J.A. & Betzig, E. Live-cell photoactivated localization microscopy of nanoscale adhesion dynamics. *Nat. Methods* **5**, 417–423 (2008).
62. Venkataramani, V., Herrmannsdörfer, F., Heilemann, M. & Kuner, T. SuReSim: simulating localization microscopy experiments from ground truth models. *Nat. Methods* **13**, 319–321 (2016).
63. Sage, D. *et al.* Quantitative evaluation of software packages for single-molecule localization microscopy. *Nat. Methods* **12**, 717–724 (2015).
64. Smith, C.S., Joseph, N., Rieger, B. & Lidke, K.A. Fast, single-molecule localization that achieves theoretically minimum uncertainty. *Nat. Methods* **7**, 373–375 (2010).
65. Egner, A. *et al.* Fluorescence nanoscopy in whole cells by asynchronous localization of photoswitching emitters. *Biophys. J.* **93**, 3285–3290 (2007).
66. Wang, Y. *et al.* Localization events-based sample drift correction for localization microscopy with redundant cross-correlation algorithm. *Opt. Express* **22**, 15982–15991 (2014).
67. Endesfelder, U., Malkusch, S., Fricke, F. & Heilemann, M. A simple method to estimate the average localization precision of a single-molecule localization microscopy experiment. *Histochem. Cell Biol.* **141**, 629–638 (2014).
68. Lin, C. *et al.* Submicrometre geometrically encoded fluorescent barcodes self-assembled from DNA. *Nat. Chem.* **4**, 832–839 (2012).
69. Bates, M., Huang, B., Dempsey, G.T. & Zhuang, X. Multicolor super-resolution imaging with photo-switchable fluorescent probes. *Science* **317**, 1749–1753 (2007).
70. Huang, B., Jones, S.A., Brandenburg, B. & Zhuang, X. Whole-cell 3D STORM reveals interactions between cellular structures with nanometer-scale resolution. *Nat. Methods* **5**, 1047–1052 (2008).
71. Shin, J.Y. *et al.* Visualization and functional dissection of coaxial paired SpoIIIE channels across the sporulation septum. *Elife* **4** (2015).
72. Puchner, E.M., Walter, J.M., Kasper, R., Huang, B. & Lim, W.A. Counting molecules in single organelles with superresolution microscopy allows tracking of the endosome maturation trajectory. *Proc. Natl. Acad. Sci. USA* **110**, 16015–16020 (2013).
73. Lee, S.-H., Shin, J.Y., Lee, A. & Bustamante, C. Counting single photoactivatable fluorescent molecules by photoactivated localization microscopy (PALM). *Proc. Natl. Acad. Sci. USA* **109**, 17436–17441 (2012).
74. Rollins, G.C., Shin, J.Y., Bustamante, C. & Pressé, S. Stochastic approach to the molecular counting problem in superresolution microscopy. *Proc. Natl. Acad. Sci. USA* **112**, E110–8 (2015).
75. Nieuwenhuizen, R.P.J. *et al.* Quantitative localization microscopy: effects of photophysics and labeling stoichiometry. *PLoS One* **10**, e0127989 (2015).
76. Sengupta, P., Jovanovic-Talisman, T. & Lippincott-Schwartz, J. Quantifying spatial organization in point-localization superresolution images using pair correlation analysis. *Nat. Protoc.* **8**, 345–354 (2013).
77. Juette, M.F. *et al.* Three-dimensional sub-100 nm resolution fluorescence microscopy of thick samples. *Nat. Methods* **5**, 527–529 (2008).
78. Broeken, J. *et al.* Resolution improvement by 3D particle averaging in localization microscopy. *Methods Appl. Fluoresc.* **3**, 014003 (2015).
79. Cheng, Y., Yifan, C., Nikolaus, G., Penczek, P.A. & Thomas, W. A primer to single-particle cryo-electron microscopy. *Cell* **161**, 438–449 (2015).
80. Szyborska, A. *et al.* Nuclear pore scaffold structure analyzed by super-resolution microscopy and particle averaging. *Science* **341**, 655–658 (2013).
81. Loschberger, A. *et al.* Super-resolution imaging visualizes the eightfold symmetry of gp210 proteins around the nuclear pore complex and resolves the central channel with nanometer resolution. *J. Cell Sci.* **125**, 570–575 (2012).
82. Penczek, P., Radermacher, M. & Frank, J. Three-dimensional reconstruction of single particles embedded in ice. *Ultramicroscopy* **40**, 33–53 (1992).
83. Perrault, S.D. & Chan, W.C.W. Synthesis and surface modification of highly monodispersed, spherical gold nanoparticles of 50–200 nm. *J. Am. Chem. Soc.* **131**, 17042–17043 (2009).